IoT Based Brain-Wave Assistive System for Paralyzed Individuals

By

Syeda Maliha Monowara
16221043
Md Ahnaf Shariar
16121078
Md. Shafayat Ul Islam
15221001
Muhammed Junaid Noor Jawad
14121044

A thesis submitted to the Department of Electrical and Electronic Engineering in partial fulfillment of the requirements for the degree of Bachelor of Science in Electrical and Electronic Engineering

Electrical and Electronic Engineering
Brac University

December 2020

Declaration

It is hereby declared that

1. The thesis submitted is our own original work while completing degree at Brac University.
2. The thesis does not contain material previously published or written by a third party, except where this is appropriately cited through full and accurate referencing.
3. The thesis does not contain material which has been accepted, or submitted, for any other degree or diploma at a university or other institution.
4. We have acknowledged all main sources of help.

Student's Full Name & Signature:

Syeda Maliha Monowara	Md Ahnaf Shariar
Syeda Maliha Monowara	**Md Ahnaf Shariar**
16221043	16121078
Md. Shafayat Ul Islam	Muhammed Junaid Noor Jawad
Md. Shafayat Ul Islam	**Muhammed Junaid Noor Jawad**
15221001	14121044

Approval

The thesis/project titled "IoT Based Brain-Wave Assistive System for Paralyzed Individuals" submitted by

1. Syeda Maliha Monowara (16221043)
2. Md Ahnaf Shariar (16121078)
3. Md. Shafayat Ul Islam (15221001)
4. Muhammed Junaid Noor Jawad (14121044)

of Fall, 2020 has been accepted as satisfactory in partial fulfillment of the requirement for the degree of Bachelor of Science in Electrical and Electronic Engineering on the 13th of January, 2021.

Examining Committee:

Departmental Head: (Chair)	______________________________ Md. Mosaddequr Rahman, Ph.D. Professor & Chairperson, Department of Electrical and Electronic Engineering Brac University
Supervisor: (Member)	______________________________ Saifur Rahman Sabuj, Ph.D. Assistant Professor, Department of Electrical and Electronic Engineering Brac University
Co-Supervisor: (Member)	______________________________ A.S. Nazmul Huda, Ph.D. Assistant Professor, Department of Electrical and Electronic Engineering Brac University
Program Coordinator: (Member)	______________________________ Abu S.M. Mohsin, Ph.D. Assistant Professor, Department of Electrical and Electronic Engineering Brac University

Abstract

Individuals suffering from severe paralysis encounter a multitude of issues that influence their quality of life. Paralysis can occur due to impairments of the central nervous system (CNS) causes by brain-stroke, accidents, neurodegenerative dysfunctions or other factors. A significant portion of our society endures the consequences that limit their physical functionalities such as movement, communication, task performances and so on. In recent decades, technology has made substantial assistive devices that can communicate the brainwave signals and interpret these into commands. The development of the brain-computer interface (BCI) depends on the electric impulses generated in the brain. Hence, this can consequently be implemented for improvement purposes, that can eventually help to overcome the aspects of functional disabilities. To resolve the obstacles associated with paralysis, this project of the brainwave-assistive system is based on the internet-of-things (IoT). The system will be further comprised of multiple sensors that continuously acquire the brainwave frequencies for implementation through the connected microcontroller.

For this project, the Cyton biosensing boards along with the WiFi shield have been utilised to read the generated electric signals from the brain which have been differentiated as per the functionality requirements. The WiFi shield enables the accumulated data to be saved in the database henceforth can be accessed at any instance (in real-time basis) through the software application. We have observed feedback generation through a microcontroller, we have further transmitted the data utilizing LSL to Python for the control of computer application. Furthermore, we intend to develop a mobile application that will frequently update the data that would enable the user to visualize the brainwave signals on a dashboard. Further research is required for a better understanding of the system to implement for extensive purposes such as home enhanced mobility, appliance control, emergency alarm-system and so forth.

Key words: BCI; EEG; FFT; OpenBCI; Bainwave;

Dedication

By the Grace of the Almighty, we have been able to manage the completion of our thesis amidst the global pandemic of COVID-19. This thesis project is dedicated to the deprived population suffering from physical disabilities and paralysis. We would be gratified to acknowledge the support of our loving parents, honourable faculties and group members.

Acknowledgement

First of all, all praise to Almighty Allah for enabling us to complete our tasks. Secondly, we are thankful to our respectable supervisor Dr Saifur Rahman Sabuj for his constant support and guidance. Furthermore, we are grateful to the Department of Electrical and Electronic Engineering, Brac University, for providing the necessary materials required for our thesis. Lastly and most importantly, we are grateful to the Department of Information and Communication Technology (ICT Division), Bangladesh Government, for generously funding our project.

Table of Contents

List of Tables

List of Figures

List of Acronyms

BCI	Brain-Computer-Interface
GUI	Graphical User Interface
MRI	Magnetic Resonance Imaging
EEG	Electroencephalography
EMG	Electromyography
ECG	Electrocardiography
CNS	Central Nervous System
FFT	Fast Fourier Transform
FIR	Finite Impulse Response
IIR	Infinite Impulse Response
RMS	Root-Mean-Square
SNR	Signal-to-Noise Ratio
LSL	Lab Streaming Layer
BPF	Band-Pass Filter
LPF	Low-Pass Filter
HPF	High-Pass Filter
RLC	Resistor-Inductor-Capacitor
DOI	Digital Object Indicator

Chapter 1

Introduction

Chapter 1 presents a sketch of the manifestation that is presumed concerning our project. Studies have been conducted on brainwaves since the mid-1900s, however, the new era is rather striving toward the implementational prospects. The innovative perspectives of neuroprosthetics and brainwave applications have accordingly been the foundational inspiration of our project. In our country, the researches based on brain-computer interface (BCI) has traditional approaches. Hence, to overcome the constraints, extensive studies are required to promote elucidation. Our project focuses on the extraction of the neural signals for assistive applications that are proposed for the greater good. However, we further plan to obtain the credentials using cost-effective tools, since the applications based in brainwaves are expensive. This chapter provides a brief discussion of the insights associated with the foundation of our project. It further designs the enterprises of the future applications of the neural signals to control assistive devices.

1.1 Background

A Brain-computer Interface (BCI) is a technological breakthrough that has managed to create a bridge between the human brain and the computer. The human brain generates electrical impulses that can be used as the input signals to a BCI system, hence, it can translate these signals into messages for the computer to understand [51]. These transmitted messages can then be further implemented as commands to perform a wide range of applications. Consequently, the brain-computer interface is often described as a mind-reading technology

[6]. However, brain activities have been read and monitored for almost a century now by devices such as EEG (electroencephalography).

Individuals suffering from paralysis and physical disabilities can perform tasks by using the signals from their brain alone [4]. For instance, BCI can be used to perform commands to enable and/or disable appliances, it can be used for operation in robotics & neuroprosthetics devices or to just write a simple text, it can even be used to control the movement of the pieces of equipment connected to it [6]. With the help of BCI, the lives of a significant number of deprived people can be improved. The main mechanism for BCI depends solely on the process of reading brain waves from an array of neurons that passes impulses through the brain's neural network [7]. The eligibility for the beneficiary, therefore, is the successful induction and transmission of sufficient neural impulses. Moreover, the use of the system Signal-to-noise Ratio (SNR) can ensure that the response is accurately transmitted through the elimination of background noises [61].

1.2 Motivation

Across the globe, there is a mounting concern surrounding the increase in the number of cases of physical disabilities and several types of paralysis. The causes of paralysis and physical disabilities are due to various factors which include brain-strokes, degenerative diseases, accidents, brain-cells damage etcetera [89]. In an era of technological advancements, the availability of tools to aid people with such disadvantages, are not available in abundance. As per the data of the World Health Organisation (WHO), about 15% of the world's population suffer from some form of disabilities at some point in their lives. However, the majority of them are generally from underprivileged communities [9]. In many parts of the world, the poor economy facilitates poorer healthcare, resulting in the percentage of the population suffering from paralysis and disabilities to be presumably higher. Among the suffering individuals who require assistive devices and equipment to function, almost 85-95% have absolutely no access to them [10]. More often than not, these people are deprived of the basic healthcare services they need due to lack of financial support [9]. Eventually causing health decline, fewer opportunities for education and work in those regions.

Although some treatments such as physiotherapy, psychotherapy, occupational, speech and language therapy are believed to show promising results, a vast number of cases remain to suggest otherwise [11]. While extensive surgeries and transplants are accessible to some victims, it might not be the case for many others. Moreover, several government organisations in associations with non-government ones are believed to provide rehabilitation centres and facilities targeted to aid the paralysed and disabled population [3]. Commonly, patients with paralysis and physical disabilities are subjected to rely on assistive or supportive devices such as wheelchairs, prosthetics, cane, etcetera [10]. However, handling these assistive devices manually can sometimes be a hassle. Since it can require physical effort, constant supervision and dependence might become an issue. Ideally, this can traverse the patients into depression and affect their mental health due to a lack of self-sufficiency [14].

Accordingly, with the inclusion of the brain-computer interface technology into the assistive system- it would require a lot less effort and might inspire a sense of independence in the patient. It will allow the patients to control and automate the movement of any connected assistive device from brain-wave signals only, for instance, a wheelchair, prosthetic arm and/or leg, etcetera. Consequently, this will not only help to restore mobility but would also prevail in the functionality of the patient. Furthermore, we can use BCI technology to control and/or command electronics and gadgets used in our everyday life. This will provide the patients with a new form of communication and control options to complete everyday tasks as well as further prepare them to be able to live on their own. It can be beneficial for individuals suffering from high-level spinal cord injury, severe neuromuscular disorders, or multiple/lateral sclerosis [49]. As of yet, there is little to no job opportunities available for people with disabilities/paralysis. We hope that with this technology, a significant number of the population that suffers can overcome the challenges and boundaries in the future. The major challenge of using the BCI system is the question of affordability.

1.3 Objective of the thesis

The prime objective of our thesis is to assist the people suffering from physical disabilities and paralysis, by solely implementing brainwave signals. With the help of the brain-computer interface (BCI) technology, the brain's neural network can be equipped to control applications. The thesis aspiration can be organised as:

- Data acquisition and visualization.
- Experimental obsevartions.
- Feedback generation and application.

1.4 Problem statement

According to the Bangladesh Bureau of Statistics, 9.1% of the total population of our country suffers from functional limitaions [12]. Eventually, this compels them to get accustomed to their conditions while affecting their mental health as well. Despite the available technological support and opportunities in developed countries, it is not widely accessible to many in Bangladesh. For a developing nation like ours, manpower is an essential contribution for economic, political and social development. Unfortunately, the deprived 9.1% of the population in Bangladesh that suffer from motor functionality, abruptly fail to continue their lives normally due to rising cases of paralysis and disability [12]. Hopefully, with the help of the brain-computer-interface mechanism, a significant amount of the deprived population can take advantage of their potential to improve their lives. However, certain factors might not always allow BCI technology to support the victims as envisioned.

For the technology to perform effectively, the input signals to the BCI network is a key factor. Therefore, the system is subjected to the generation of brain wave signals in the optimum frequency range. In the case of paralysis, such signals are inherently developed in the brain, however not successfully transmitted through the spinal cord. Similarly, for cases of disabilities at a certain part of the body, brain wave signals are also generated as presumed. Whereas, in some if not most victims, the collected brain wave signals may not always be optimum. Patients suffering from brain injury, stroke, aneurysm or neurological illness, commonly have damaged nerves/neurons and therefore, might not be able to benefit from the BCI technology. Thus, the electrical impulses generated in their brains are often inadequate to be utilised in the BCI. Correspondingly, this can disrupt the BCI system from functioning as anticipated. On that account, the support of diagnostic tests and/or pieces of equipment used for mapping the brain readings, can often be useful to verify the efficiency of the generated brain wave signals.

1.5 Methodology

The principal idea is to accomplish affirmative outcomes using the BCI technology and to ensure this, the condition of the subject's brain ought to be analysed by neuroimaging. Consequently, mapping and analysing the brain's neural pathways through diagnostic tests such as EEG (electroencephalography), EMG (electromyography), MRI (magnetic resonance imaging) or fMRI (functional magnetic resonance imaging) can be quite beneficial.

Henceforth, our project includes cyton-daisy biosensing board which focuses on extracting and reading the EEG and EMG data in a non-invasive method [19].

Albeit the data is collected in real-time, but can also be stored for further modification and utilisation. Additionally, we can continuously observe them in graphical form with the help of the OpenBCI GUI application. The data signals are then filtered and sampled accordingly for a farther specification. Moving forward, the filtered signals are interfaced with applications such as Python and Arduino by LSL and serial communication. These applications can be designated for the implementation of the processed data signals into commands and outputs. Eventually allowing the user to perform tasks instantly through continuous streaming of data in real-time. For instance, a motor car can be favourably controlled, home-appliance automation can be executed, completing small tasks on computers and tablets such as scrolling and slide control.

1.6 Overview of the contents

Chapter 1 illustrates the background of our project and provides details of the brain-computer interface (BCI) technology. Our project aims to aid people suffering from paralysis and physical disabilities. Hence, with the help of BCI and its beneficial features, our motivation is illuminated.

Chapter 2 mainly covers the features of the human brain and its organization. It essentially focuses on the construction of the brain and the impairments that can disable the central nervous system (CNS). It further discusses the several techniques for the observation and investigation of the brain. The focal details for the generation of the brainwave signals to read brain activity are also elaborated.

In chapter 3, we have discussed the details of hardware and software that have been utilised for our project. The specifications of the components are provided along with their configurations. The explanation on MATLAB, Python and OpenBCI GUI applications incorporates how each served a purpose in our project at different instances.

In chapter 4, we have concentrated on the theoretical and mathematical perspectives of our project. The discussions include the computational analysis and the theories that apply to our project. This section emphasizes on the thesis model that made the practical implementations possible.

Chapter 5 entirely focuses on the results, observations and the outcome of our project. This chapter is the practical perception of that of the previously established chapters. We have conducted several experimental studies to deduce that brainwave can alone control a system if administered intricately. Upon this deduction, we have implemented the collective brainwave signals for focus-control applications of robotic car and scrolling of computer newsfeed.

Lastly, chapter 6 comprises the overall constraints faced and the future aspirations of our project. It also concludes our perspectives and learnings of the thesis project.

1.7 Literature review

Vinoj et al (2019) proposed a framework to utilize a brain-controlled lower limb exoskeleton (BCLLE) where the user controls the movements. It implements a flexible design which is can be modified based on the degree of physical disability [1]. The BCLLE system, which is modelled after the human anatomy, can identify the status of the paralyzed individual and can securely transmit information to caregivers in case of emergencies through Novel-T Symmetric Encryption Algorithm (NTSA) [1]. An electroencephalogram (EEG) headset captures human intentions based on the signals acquired from the brain waves of the user to control the motors of the exoskeleton. The brain wave signals are converted into digital data using the brain-computer interface while these are interfaced with the motors through a microcontroller which controls the high torque motors connected to the exoskeleton's joint depending on the user's purpose. In comparison to existing solutions, the classification accuracy of this proposed method is much higher at more than 80% [1].

On a similar account, Navitasori et al (2020) conducted similar experiments to find the most stable EEG parameters for observation of rehabilitation. The parameters were found by measuring the difference between the values of the features of healthy hand movements in contrast to the movement of that of the affected hand, in the same individual stroke patients [2]. The study was conducted on 10 stroke patients who were monitored while performing three variations of hand movements. This primarily focused on shoulder flexion-extension, elbow flexion-extension, and grasping on both healthy and stroke-affected sides. For further EEG processing, IIR was applied at the band-pass filter stage, which was followed by ASR and ICA algorithm to remove artefacts [2]. After comparing, the difference between the healthy side feature (HFV) and the affected side feature (AFV) the study concluded that STD, during shoulder movements, and in low Alpha range of frequencies provided the best feature with the most positive HFV and AFV differences. Henceforth, this concluded the implication of voltage or action potential of the brain as a crucial parameter in case of stroke rehabilitation progress [2].

Chapter 2

The Human Brain

This chapter mainly constitutes of the neurological and the neuroscience-based perspectives of our project. Detailed analysis of the human brain is correlated to the conditions of paralysis and physical disabilities. Further presented, the features of analysing the required attributes for the successful execution of our project.

2.1 Fundamentals of the brain

The human brain is the individual organ which is responsible for controlling the entire body. An average human brain weighs about 1.5 kg and/or represents 2% of the body mass; it consists of over 86 billion of packed neurons and neurotransmitters [25]. Our brain is responsible for transmitting information conducted by neurons and neurotransmitters in the form of electrical signals. It is the essence of our central nervous system (CNS) and is inherently the source of human intelligence and functionality [22]. The brain facilitates and controls every human feature. It is solely responsible for perceiving complex emotions, cognitive thinking, problem-solving, performing tasks, movement and stability, communicating responses, regulating nutrients and hormones, controlling breathing, etcetera [28].

The brain requires a constant accumulation of glucose because it is the essential source of energy for the support of brain digestion system and work [27]. On average, the brain consumes about 15% of the cardiac production and 20% of all the energy in a human body, and that too, while the body is at resting state [25]. However, it has also been discovered that 60-80% of the overall energy expended by the brain is employed in neural signalling since the brain is continually active [27]. The energy consumption increases an additional 5% when performing tasks, hence, maximum consumptions occur for intrinsic functionalities [44]. The functionality of the different domains of the brain is envisioned as a polyhedron, each with diverse attributes [23]. The major structures of the brain are the cerebrum, the cerebellum, the diencephalon (which consists of the thalamus, hypothalamus and pituitary gland), and the brain stem (that includes the midbrain, pons and medulla) [22].

The main regions of a brain:

- The brain stem.
- The cerebellum.
- The cerebrum or cerebral cortex.
  - Left hemispehere.
  - Right hemisphere.

Each hemisphere consists of the frontal lobe, the temporal lobe, the parietal lope and occipital lobe. Each of these lobes have unique, yet essential functions.

2.2 Brain functionalities

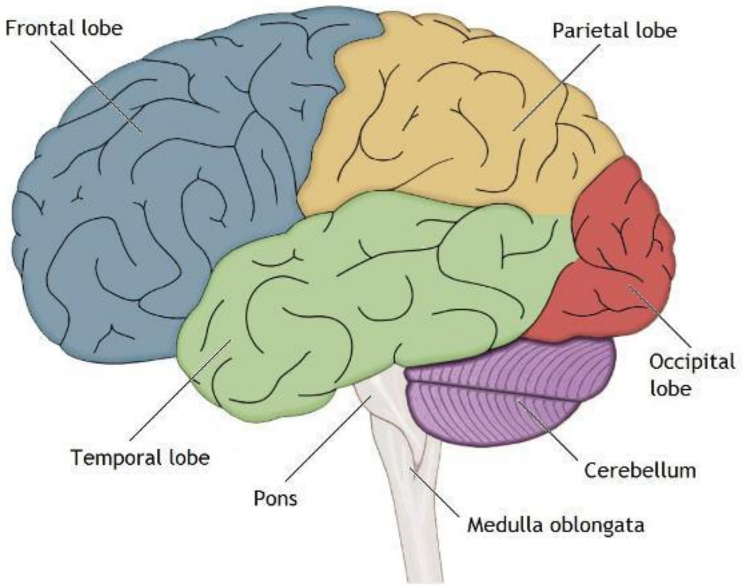

Figure 2.1: Cross-sectoinal area of the human brain [78].

2.2.1 The cerebrum

The cerebrum, frequently known as the cerebral cortex, occupies the largest surface area of the brain due to the numerous folds and convolution of brain matter. This entire part of the brain controls our communication, conscious and unconscious thinking, sensations, perceptions, actions, vision and other senses [21]. The cerebrum is ordinarily partitioned into two hemispheres, the left and the right hemisphere. Additionally, the two hemispheres are interconnected by the bundle of nerve fibres called the corpus callosum. Usually, the left hemisphere controls the right part of the body, whereas, the right hemisphere controls the left. This means that damage to the left hemisphere due to a stroke, for example, can lead to paralysis on the right side of the body. The right cerebral cortex is usually effective for spatial rationalising or description. Whereas, the left is responsible for speech and intellectual thinking in most people [22]. Nevertheless, the cerebral cortex is further segmented into several regions based on their molecular and biological characteristics. Thus leading to the expansion of different functional networks [23]. Ordinarily, the two hemispheres are classified into four sections or lobes, each with a designated function of its own. They are the frontal lobe, the temporal lobe, the parietal lope and occipital lobe [78].

The frontal lobes are the largest of all the lobes and positioned directly behind the forehead. These lobes are fundamentally responsible for controlling communication, behaviour, knowledge, judgement, concentration, motor-function, personality, self-awareness and various cognitive aspects [26].

The temporal lobes are located near the foundation of the skull and are imperative for the social brain. They are usually in control of the hearing, memory, and communication features in a person. Temporal lobes enable individuals to comprehend languages in written form or speech and responsible for the qualities of sequencing and coordination. Moreover, it also helps with the recollection of memory and emotions [25].

The parietal lobes are located at the centre of the brain, between the frontal and occipital lobes. These lobes are essential for interpreting different senses such as sensory comprehension, vision, hearing and touch. These lobes are also responsible for language and memory functions, as well as visual and spatial observations [78].

The occipital lobes are the smallest lobe of the cerebrum. The principal function of the occipital lobe is to perceive and interpret optical information. Consequently, these lobes allow detection of light, colour, the motion of an object, etcetera [26].

2.2.2 The cerebellum

The cerebellum is the largest of the hindbrain and an essential element of the human brain. It is responsible for motor-movement, coordination, posture and balance maintenance. The cerebellum also controls several cognitive capabilities such as attention, language, fear, stress, pleasure and human reactions. Although the cerebellum itself does not cause muscle contraction, it contributes to the refinement and precision of locomotive action by controlling voluntary muscle activities. Hence, any harm to this particular region can affect in a loss. It can consequently impair the capability of controlling precise movements, motor learning, maintaining posture and balance. Furthermore, the cerebellum connects to the brainstem by three assortments of nerve fibres called the superior, middle, and inferior cerebellar peduncles, through which it farther connects with the rest of the nervous system [28].

2.2.3 The brain stem

The brain stem is located at the bottom of the brain. It connects the cerebellum and the spinal cord to the cerebral hemispheres and transmits information amongst them. The brainstem includes the midbrain, the pons and the medulla. The brain stem is responsible for maintaining fundamental body functions such as breathing, hearing, vision, balance, blood pressure, pulsation, etcetera. It further controls eye movements and facial expressions [21].

The brain stem can be categorised into four different segments: the diencephalon, midbrain, pons and medulla oblongata. The most superior part of the brainstem is the diencephalon. It is further segmented into four portions that include the epithalamus, subthalamus, hypothalamus and thalamus. The largest portion of the diencephalon is the thalamus. It is essentially regarded as the relay point, where all the sensory data is being registered, transmitted and further processed. The thalamus provides the cerebrum with sensory information from the target regions of the skin, eyes and ears. Nevertheless, the hypothalamus normally regulates the basic requirements of the biological traits such as thirst, hunger, body temperature, sleep patterns and sexual behaviour. Besides, along with the pituitary gland, the hypothalamus also controls the secretion of hormones in our body [24].

As we know, the midbrain routinely calculates the visual observations and movements. However, the hearing and balance of the human body are controlled by the pons. The pons furthermore controls the sensory data associated with the facial nerves such as eyes and facial alterations. The most miniature portion of the brainstem is the medulla oblongata. By and large, it governs the fundamental capabilities such as breathing, palpitation, cardiac rhythms and gulping. The collapse of the medulla oblongata is ideally considered as brain death of patients in clinical terms [24].

2.3 Paralysis and physical disabilities

Physical disabilities and paralysis go hand in hand regardless of the modernization of our societies all over the world. Disability is a colossal concern that threatens the public health as well as the economy of every nation. It is estimated that 15% of the total world population suffers from some form of disability, among which, 80% belong to the developing countries [12]. According to the United Nations Convention on the Rights of Persons with Disabilities (UNCRPD, 2006), an individual with any form of mental or physical impairments lasting over a prolonged period of time can be asserted to suffer from disabilities [12]. Physical disabilities, be it due to unavoidable causes or preventable one, causes an afflicted life. For instance, the cases of physical disabilities may vary from unforeseen circumstances of accidents, injuries and amputations to those caused by inherent dysfunctions.

On the other hand, paralysis occurs when there is an abruption of connection in the central nervous system (CNS) of the human body. The CNS is comprised of the brain and the spinal cord. Thus, any destruction or interruption in the CNS network prohibits the neurotransmitters to successfully transmit the brainwave signals [25]. Although the brain might be continually generating the brainwave signals as anticipated, paralysis hinders the muscular movements and physical bodily functions. Loss of muscle control is due to the inadequacy of the neural circuitry [15]. According to the survey conducted by the centre for disease control and prevention (CDCP), the significant causes of paralysis are as follows [89]:

- Brain stroke.
- Spinal cord injury (SCI).
- Brain or spinal cord tumours and infections, meningitis.
- Motor neuron dysfunction.
- Cerebral palsy (CP).
- Degenerative diseases such as Multiple sclerosis (MS).
- Autoimmune diseases such as Guillain-Barré syndrome and Lupus.
- Brain or spinal cord tumours and infections, meningitis.
- Spina bifida (deficiencies during birth), incomplete development of the CNS.

2.3.1 Types of paralysis

Most commonly, stroke results from a blood clot in the brain causing the blood vessel to burst and bleed in the brain. This causes interruption of blood flow to the regional brain, leading to neuronal destruction that can lead to various neurological disorders including paralysis [25]. Paralysis can vary to certain degrees, severity and types. For occurrence, paralysis can be permanent, temporary, partial, complete, flaccid or spastic [15]. In milder cases, such as flaccid, where the muscles become lax and shrivel up; or spastic, where the muscles become tight and move with sudden and unintentional jolts [14]. Generally, localized paralysis affects only a particular segment of the body like the face, feet, hands, vocal cords, etcetera [15]. Complete paralysis occurs when one loses the ability to control any part of the muscles, this can either be permanent or temporary. Permanent paralysis cannot be treated, however, there are treatments available for temporary paralysis [14]. Majority of these treatments are forms of rehabilitation that include physical therapy, occupational therapy, speech therapy and functional electrical stimulation. Moreover, assistive and mobility devices such as wheelchairs, braces, canes, any wearable electric devices are often effective [11].

However, the generalized paralysis is commonly broken down into numerous categories. Theses include monoplegia, hemiplegia, paraplegia, diplegia and quadriplegia [15]:

- Monoplegia generally applies to paralysis that develops only in one limb (arm or leg).
- Hemiplegia refers to paralysis on one specific side, affecting the limbs of the corresponding side of the body (left or right).
- Whereas, diplegia targets the same parts of the opposing sides of the body (both arms/legs).
- Paraplegia frequently attacks the bottom half of the body.
- Lastly, quadriplegia influences more extensive perimeter of the body. It is concerned with paralysis of both arms/legs, from the neck and downwards while harming other organs as well.

2.4 Analysis of the brain waves

2.4.1 Brain Waves

The brain has billions of neurons and neurotransmitters that conduct transmissions through electric stimuli. These neurons in the human brain obtain electric signals from thousands of other cells for sustaining suitable response mechanism [16]. The study of neuroscience has traditionally relied on analyses of the membrane potential using electrodes due to the course of conduction being electrical [17]. Synchronised neuro-transmissions induced by electric impulses within the neural networks in the brain, invariably produces neural oscillations known as brain waves. Brain wave is a generic term extensively used to refer to the electrical or neural impulses generated in our brains. The broadly dispersed pathways of neural fibres, facilitate omnidirectional transmissions of the brain waves [18].

Brain waves can subsequently be measured and observed with instrumental techniques such as electroencephalogram (EEG). The word encephalon is derived from a Greek letter which means within the head. Customarily, readings are taken using conductive electrode-caps attached to the exterior surface area of the head. This is the most approachable procedure since it is not an invasive one. The EEG brain waves are procured in oscillations and determined in cycles varying with time, known as frequencies. The range of frequencies of the brain waves is measured in the unit of Hz (hertz) [29].

2.4.2 Types of brain waves

The brain waves are ordinarily in a low range of frequencies. They are categorised into five groups, each with corresponding attributes. On account of neural activities, the brain waves are classified into Delta, Theta, Alpha, Beta and Gamma waves [40].

Rhythm	Mental condition	Consciousness	Wave pattern
Gamma 40 – 100+ Hzinformation processing	Cognitive functioning, learning	Very high	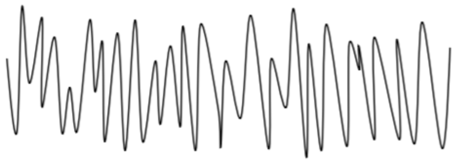
Beta 12 – 40 Hz	Attentive, problem solving, judgment, decision making	High	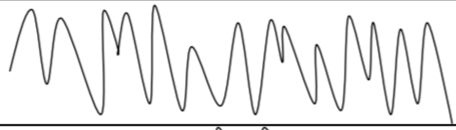
Alpha 8 – 12 Hz	mental coordination, alertness, calmness	medium	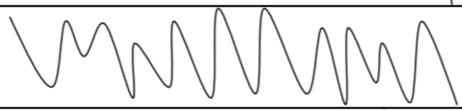
Theta 4 – 8 Hz	Deeply relaxed, semi-hypnotic state	low	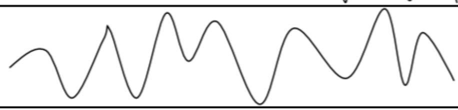
Delta 0.5 – 4 Hz	Dreamless sleep, meditation	very low	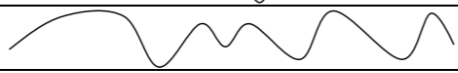

Figure 2.2: Brainwave rhythms [30].

1. Delta brain waves (ranges 0.5 – 4 Hz):

They are graphed as the slowest brain waves with a frequency range of 0.5 Hz to 4 Hz. Delta brain waves are experienced during the most profound state of sleep or meditation [72]. On the other hand, delta consists of the highest amplitudes and are incorporated with dominant brain wave categories. These are often generated when we are in a complex form of consciousness, such as dreamless sleep [40].

Nonetheless, sufficient generation of delta brain waves is essential. For instance, monitoring unconscious biological functions such as regulating heartbeat and digestion. Furthermore, they are vital for the restoration and rejuvenation of the body. Be it to recover from severe illness/injury or general tiredness. Perversely, unusual delta brain waves can create hurdles in managing consciousness. It can further affect learning and comprehensive capabilities [30].

2. Theta brain waves (4 – 8 Hz):

Theta brain waves generally occur during deep meditation or in a state between sleep and waking, often regarded as dreaming. Considering relaxed brain activity, it is related to learning, recollecting memories and feeling emotions [30]. Throughout theta brain activity, our sensations are rather centred than focusing on the surrounding. Hence, it can enhance our creativity, foreknowledge and be therapeutic [72].

3. Alpha brain waves (8 – 12 Hz):

Alpha brain waves are visibly larger in scale and slower in comparison to the other brain waves. Their frequency range is between 8 to 12 Hz, that is between the Theta and Beta ranges. Alpha waves are affiliated with a state of moderate consciousness. Hence allowing a sense of tranquillity and calmness such as when in sleep [40].

Alpha brain waves act as a passage between the subconscious and the conscious mind. This can be beneficial for mental wellness, achieving a mind-body attentiveness and profound relaxation [30].

4. Beta brain waves (12 – 40 Hz):

Beta brain waves are perceived in our general state of waking, alertness and consciousness. They are associated with mental, intellectual, analytical and cognitive activities. The appropriate balance of Beta waves is presumably efficient for problem-solving tasks. More often than not, a disproportion of Beta waves can stimulate unpleasant feelings such as stress and/or anxiety. Regardless, they are undoubtedly favourable for social performance and the conscious mind [30].

5. Gamma brain waves (40 - 100 Hz):

Gamma brain waves are detected at the extreme level of consciousness and intricate cognitive functions. They are graphed as the most complex brain waves with the highest frequencies, ranging between 40 and 100 Hz. Gamma waves incorporate improved cognitive functions, processing of information, empathy, alertness and mindfulness. Thus, these are regarded as the optimum frequency for the functionality of the brain. Individuals suffering from disabilities tend to have lower than average Gamma wave activity. Therefore, causing extreme distress and challenges in learning and memory [30].

2.4.3 Benefits of brainwave analysis

Thereupon, brain waves research and implementation have various prospectuses. To accomplish a brain-computer interface with brain waves, the Beta range of frequencies (12-40 Hz) is the most suitable of all. It can be the optimum selection for controlling devices and interfaced applications. Since it is a state of natural alert consciousness, thoughts and commands are clearly conducted [20]. Furthermore, studies of the lower frequencies of brain waves undeniably yield outcomes concerning mental and emotional health. Monitoring brain waves can precedently assist with the prognosis of dysfunctions in the human mind and body. Individuals suffering from conditions of learning disabilities, ADHD, Tourette’s syndrome, head injury and stroke- often possess unusual ranges in the Alpha and Theta brain waves [40]. Invariably, Alpha brain waves are popularly associated with the research of attentiveness. The detection of slower brain waves at the frontal lobe is correlated with issues related to concentration, memory, behaviour, hyperactivity and so on. Alpha waves factually oscillate in the frequency range of 8-12 Hz, are supposedly responsible for filtering out perplexed neurological signals. Thus, analyzing and controlling its stability can persistently improve the attention capacity in individuals [41].

2.4.4 Methods of neuroimaging

Brain imaging evaluates the neurological signals that help determine the underlying physical, mental and psychological aspects. Brain imaging can be effortlessly accomplished through unique approaches that read the non-invasive brain wave signals, rather than performing incisions. These include electroencephalogram (EEG), magnetoencephalography (MEG), functional near-infrared spectroscopy (fNIRS), magnetic resonance imaging (MRI) and functional magnetic resonance imaging (fMRI). Considering the position of the cerebral hemispheres, the signals accumulate over the surface area of the head. Thus, the manifestation of the proclaimed brain wave signals is considerably accessible. Hence, the electrode-caps are attached on the forehead and all over the scalp to acquire active readings [51].

1. Magnetic Resonance Imaging (MRI):

Magnetic resonance imaging (MRI) implements the potent magnet, radio waves in cooperation with the computer. In the mechanism of MRI, the magnetic field generally corresponds with the proton elements in our body. Since our body consists of 70% water, the magnetic field targets the hydrogen atoms arbitrarily and examines its contents. The emitted frequencies of radio signals from MRI further interacts with the proton elements for a brief moment. Upon relaxation of the elements to their regular state, the energy discharged is instantly identified by sensors in the MRI device. Correspondingly, MRI produces detailed static imaging of the anatomy of the brain circuitry [42].

2. Functional Magnetic Resonance Imaging (fMRI):

On the other hand, the process of functional magnetic resonance imaging (fMRI) depends on the level of oxygen content rather than that of water. Initially, the emitted energy from the alteration of the proton elements in brain tissue is analysed. Thereupon the blood oxygen level-dependent (BOLD), transported by the haemoglobin molecules in the bloodstream [19]. The iron content of haemoglobin molecules exhibits magnetic properties while carrying oxygen molecules. Thus, even the slightest of variation can be derived. Ordinarily, the brain contains a great level of oxygen in regions with high activity. The fMRI distinguishes the variation in magnetic properties and yields three-dimensional images in response to brain activities [43].

3. Electroencephalography (EEG):

The electroencephalography (EEG) is evidently the most widely used diagnosis for determination of brain wave signals. Due to the advantages of high portability and cost-efficiency, EEG signals have drawn considerable attention. Majority of the modern research on non-invasive brain signals are related to EEG [51]. Furthermore, it requires little to no preliminary training. It is also suitable for direct and continuous detection of brain waves signals in real-time, unlike the static features of the other techniques [42]. EEG obtains brain waves in response to stimulation of sight, sound, or touch. It further distinguishes anomalies in the electrical activity of the brain signals. Hence, it can be valuable for investigating neurological dysfunction, emotion mapping, etcetera [45]. The electrical impulses in the brain move in all directions, hence we can get hold of these signals non-invasively through sophisticated electrical charge amplifiers [18]. For this process, multiple miniature metal electrode-caps are attached across the scalp and on top of the forehead through a conductive paste [45]. The electrodes follow the technique of electroencephalography and attract charges from brain cell activity [18].

Initially, EEG examines the variation in these charges resulting from the ionic current. The quality of the assembled brain wave signals remains immensely affected due to the presence of impediments- the skull and meninges, between the electrode-caps and the scalp surface [51]. Theoretically, the accuracy calculated by Signal-to-Noise Ratio (SNR) of the obtained brain signals to that of the originated ones is approximately 5% [47]. Generally, the obtained signals are processed for noise reduction and sampled using frequency-domain Fourier transformation. Accordingly, the decoded brain signals can be implemented in the brain-computer interface (BCI) system to be transformed into digital commands. Thus the brain signal-based applications can directly serve the user without any time delay. This can allow the user to control smart equipment, home appliances and external assistive devices such as a wheelchair, robotic arm and robots. People suffering from psychological or physical disabilities can use brain wave signals to function for their daily life [51].

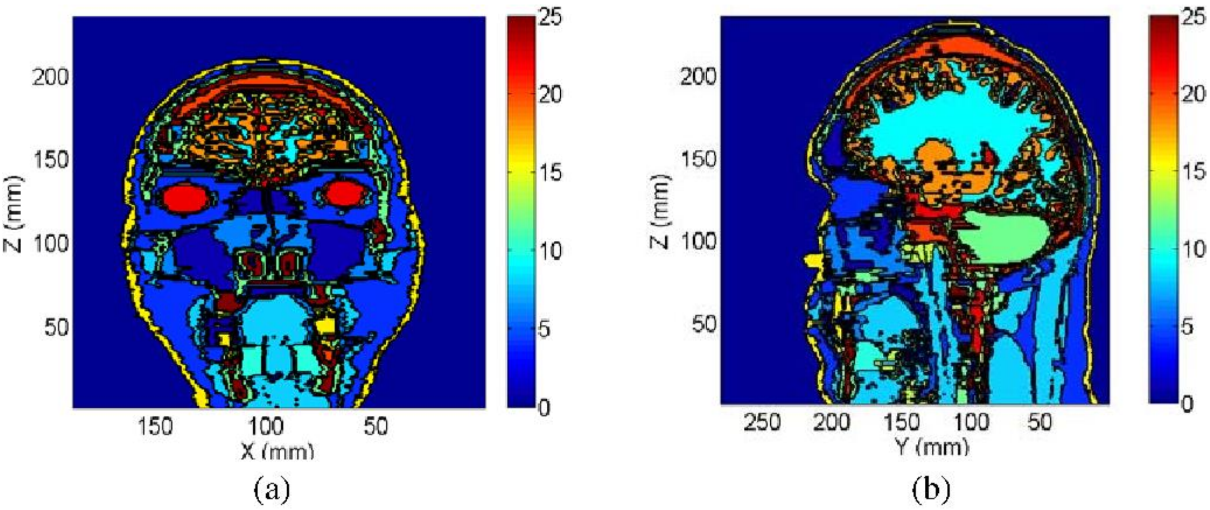

Figure 2.3: The distribution of brain activity observed during invasive EEG for two sections of the head. (a) X-Z plane, (b) Y -Z plane [20].

Chapter 3

Hardware and Software

3.1 Hardware components

3.1.1 Cyton Biosensing Board (8 Channel)

The OpenBCI Cyton Board is an 8-channel neural interface which has a 32-bit processor and is Arduino compatible. The OpenBCI Cyton Board utilizes the PIC32MX250F128B microcontroller which ensures that the data is received at fast speed while also ensuring high speed data processing utilizing it’s own local memory. The OpenBCI firmware is preloaded with the board where each of the 8-channel data is sampled at 250 Hz [31].

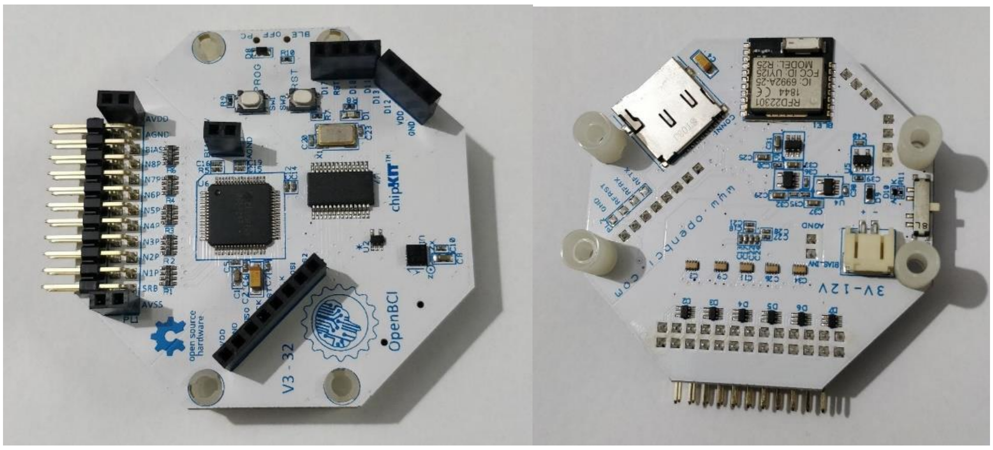

Figure 3.1-3.2: Cyton Biosensing Board (Top and bottom face).

Using this board, it is possible to receive brain activity (EEG), muscle activity (EMG) and heart activity (ECG). This board has wireless communication features which enbles it to communicate with a computer or any external hardware such as Arduino, Raspberry Pi etc. using RFDuino and Wi-Fi Shield. Furthermore, it can also establish wireless communication with any Bluetooth low energy compatible mobile or tablet [31].

Power	~3.3-12V DC Battery
Chip	PIC32MX250F128B with ChipKIT UDB32-MX2_DIP bootloader
SRAM	32 KB
Flash Memory	3KB
Clock Speed	50MHz
ADC	Texas Instruments ADS1299ADC
Channel Resolution	24-bit Channel
Programmable Gain	1,2,4,6,8,12,24
Digital Operating Voltage	3.3V
Analog Operating Voltage	+/-2.5V
Accelerometer	LIS3DH
Storage	SD Card
GPIO Pins	5 pins, 3 of which can be analog

Table 3.1: Cyton Board Specification [31][32][33].

Cyton Data Transmission and Format

The data transmission initializes as the Cyton board begins to send single ASCII b data. Upon receiving the transmitted data, continuous data transmission commences which is transferred in the binary format. The data transmission is halted when it sends s as command [34].

Each transmitted data contains a header along with a sample counter followed by 8 ADS channel data with 3 axis value of the accelerometer concluded with a footer. A typical representation of the data during the transmission is shown below [34].

Header	Byte 1: 0xA0
Byte 2	Sample Number
EEG Data	Bytes 3-5: Channel 1
Bytes 6-8	Channel 2
Bytes 9-11	Channel 3
Bytes 12-14:	Channel 4
Bytes 15-17	Channel 5
Bytes 18-20	Channel 6
Bytes 21-23	Channel 7
Bytes 24-26	Channel 8
Aux Data	Bytes 27-32: 6 bytes
Footer	Byte 33: 0xCX

Table 3.2: Data transmission method [34].

3.1.2 OpenBCI Dongle

Module	RFD22301 Radio Module
UART	FT231X USB to serial converter

Table 3.3: Dongle Specification [35].

This dongle funtions as a communication medium between the host computer and the device where the dongle is connected in the USB port of the computer. The dongle is featured with single chip USB to asynchronous serial data transmission which has a true 3.3V CMOS drive output and TTL input. Additionally, it can support the UART interface support for 7-8 data bits with 1 or 2 stop bits along with odd/even parity [35].

Figure 3.3: Cyton Dongle RFDuino.

3.1.3 Wi-Fi Shield

The Wifi shield is s ESP8266 based module which is compatible with Arduino, Raspberry Pi. It provides the opportunity to transmit data through HTTP wifi server from where the data can be stored into the database and can later be visualized in OpenBCI GUI [36]. Adding to that, it is possible to obtain low latency high reliability wireless data transmission by using a TCP socket from the computer which is transmitted from the wifi shield [37].

The streamed data obtained from the wifi shield can be stored into json format which opens door to many possibilities such as web implantation, application implementation [37].

Figure 3.4: Wifi shield.

Power	3.3V - 6V DC
Current	150mA
Frequency Range	2.4GHz – 2.5GHz
Protocol	802.11 b/g/n
Security	WPA/WPA2
Power Input Type	JST Power

Table 3.4: Wifi shield Specification [38].

3.1.4 Gold Cup Electrodes

In general, gold cup electrodes are attached to the scalp of the test subject and electrode paste ensures a secure connection to the head. These gold cup electrodes can have pure silver with gold plating or either only silver plating or only gold plating [80]. The purpose of the silver or gold plating is to provide better conductivity. Unlike electrode cap, gold cup electrodes can be used as many times as required as it is easier to clean after use. Using gold cup electrodes, it is possible receive data such as EEG, EMG and ECG [81].

Figure 3.5: Gold Cup electrodes.

3.1.5 Ten20 Conductive Paste

Conductive paste is used before the EEG electrodes are attached to the test subject's head. Adding a little scoop of paste into gold cup electrodes provides for better conductivity and secure connection with the scalp. Spreading more area on the gold cup will result in better results as there will be an increase the amount of data receive from the scalp using the electrodes. The scoop of the paste is applicable for one time use only and is required to be cleaned up with cotton and warm water from the surface of the gold cup electrodes after a single usage. The Ten20 Condcutve paste is compatible with any kind of gold cup electrodes [82].

3.1.6 Electrode Cap

The electrode cap is used to observe EEG reading from subject's head. One of the key features of the electrode cap is that it is made following the 10-20 system while it's electrode placement is much more accurate than the traditional gold cup electrodes as well. Thus it provides more thorough and accurate data. Unlike gold cup electrodes, electrode cap enables the user to utilize upto 19 channel and it can also be interfaced with the Cyton board using touchproof adapter cable. The electrode cap comes with following two different options (1) Ag/AgCl coated electrodes and (2) sintered Ag/AgCl electrodes [5].

Figure 3.6: Electrode Cap.

3.1.7 Electrode Cap Gel

The electrode cap gel is used on the electrode cap which works similarly to the Ten20 Conductive Paste. The only difference is that rather than directly applying the gel on the electrode cap, it is applied using a syringe. The use of electrode cap gel is intended for only wet electrode EEG cap [83].

3.1.8 EMG/ECG Foam Solid Gel Electrodes

Solid Gel Electrodes are disposable electrode to be used while receiving data from any muscle or heart activity and is intended for one time use only. It is a solid gel over a foam surface where aqua-tac adhesive used to stick it on skin. This can also be used for EEG but it is not recommended as it shows much greater adhesion [84].

Figure 3.7: EMG/ECG Foam Solid Gel Electrodes.

3.1.9 EMG/ECG Electrode Snap Cables

EMG/ECG electrode snap cables can only be used with disposable EMG/ECG gel. Snap cables are easy to connect with the Cyton board to receive EMG/ECG activity [85].

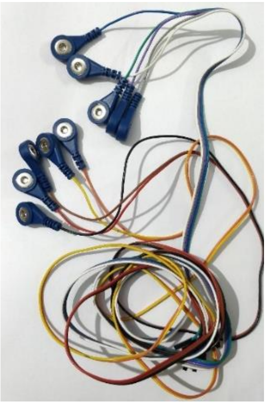

Figure 3.8: Electrode Snap Cables.

3.1.10 Motor Driver L298N

L298N motor driver is a high current dual full bridge motor driver which can endure high current and high load and is compatible with Arduino for controlling DC motor. It can be interfaced with solenoids, relays, stepper motor, inductive load and DC motors. Moreover, motor driver can tolerate maximum voltage up to 50V where the output current and the peak current is up to 3A [87].

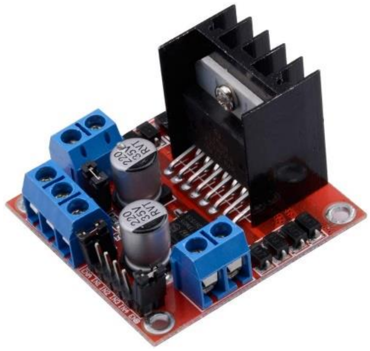

Figure 3.9: L298N Motor Driver [86].

Power Supply	5-50 V
Logic Supply Voltage	7 V
Enable Voltage	-0.3 – 7V
Peak Output Current	3A
Power Dissipation	25W

Table 3.5: Motor Driver Specification [87].

3.2 Software

3.2.1 OpenBCI GUI

The OpenBCI GUI is the key software for this project as this software enables us to visualize, record and stream data from the Cyton board to the external hardware and software. The OpenBCI GUI is highly customizable to properly serve the requirements according to user preference. Moreover, the recorded data can be saved and played back as per the user's requirements while it can also be saved into text file format for later use [88].

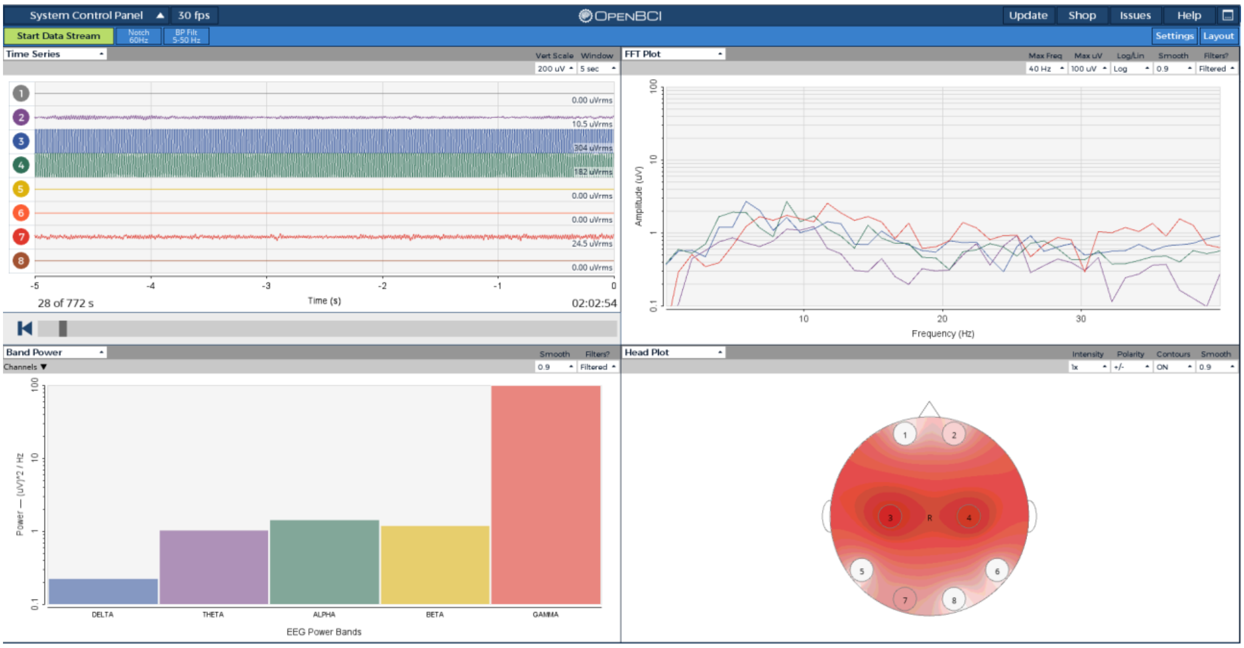

Figure 3.10: OpenBCI GUI observation.

3.2.2 Python

Python provides a great number of use while working with the data stream from brain activity of the test subject. The GUI enables the user to transmit the data received through the Cyton board via LSL to python. Moreover, data received in python can be used to visualize the raw unfiltered EEG data. Python enables the user to utilize these data to create programs which can implement various types of task as per requirement such as, Web application data stream, Machine Learning to predict the body movement from brain activity, performing task on computer such as scrolling, mouse cursor control and so on. Data can be transmitted to python via two ways, the first method is using the LSL from the GUI and second is from the HTTP server through wifi shield [48].

Chapter 4

Data processing and Optimization

In this chapter, the theoretical aspects of our thesis model are elaborately presented. The aspirations and analysis for the embodiment of the project are primarily focused. Detailed discussions and mathematical equations that have been employed by the technological segments are extended.

4.1 Data Receive Methodology

4.1.1 EEG analysis and implementation

In Chapter 2, we had previously discussed how brainwaves are produced in the form of electric impulses/signals due to neurotransmission. The signals are measured from any point on the scalp surface using non-invasive EEG techniques since they are omnidirectional in nature [44]. Furthermore, we have manifested the beneficial purposes of Electroencephalography (EEG) technique and how it can be appropriated for Brain-Computer Interface (BCI). The Cyton-biosensing board is one such instrumentation which in addition to the OpenBCI open-source platform, provides the functionality in a relatively similar composition [18]. In our project, the Cyton-biosensing applies the mechanism of EEG and simultaneously detects the electric impulses from the brain. The electrode-caps placed on the surface of the scalp attracts and captures the electric impulses for further implementation. This phenomenon has been enabled because the impulses are electrical/ionic charges with a difference in membrane potentials [17].

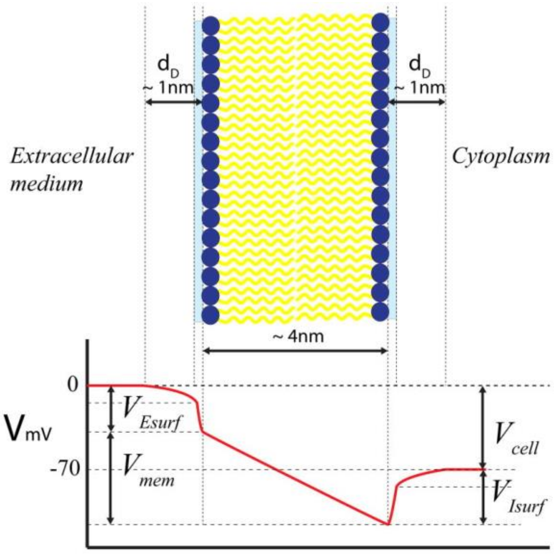

Figure 4.1: Action potential curve [17].

Consequently, this exhibits the electrical attribution of the nerves and are occasionally termed as the action potential. Upon stimulation and functional activity, the action potential changes phases with changing potential of the membrane [17].

The initial rise in potential from the state of resting potential is called hypo-polarization. A further rise in the potential causes the cells to become increasingly electropositive. However, this phase is termed depolarization. Upon reaching a peak of extreme electropositivity called overshoot, the potential decreases and repolarization occur to restore the resting potential. However, a state of hyperpolarization is achieved due to the negative potential values (ionic charges). Soon after that, the membrane potential is re-established for the action potential to deliver repeatedly [53].

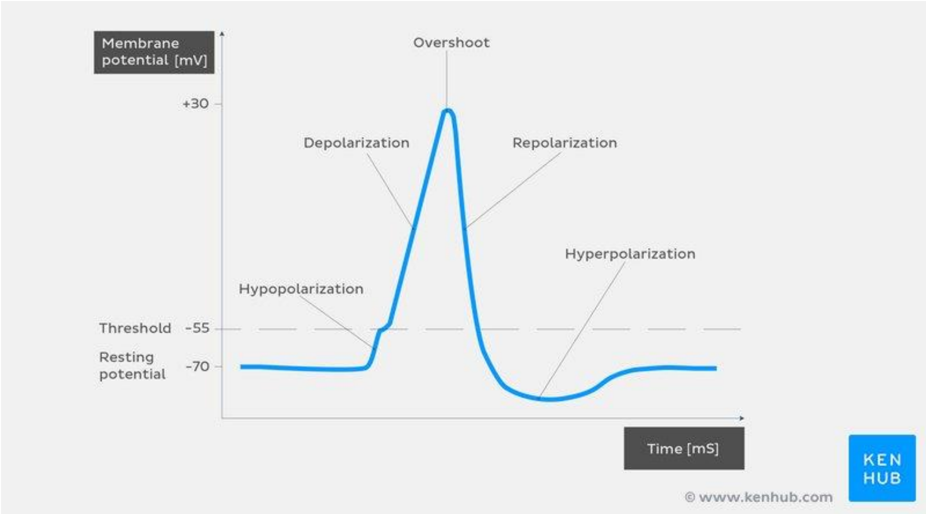

Figure 4.2: Action potential curve at different stimuli phases [53].

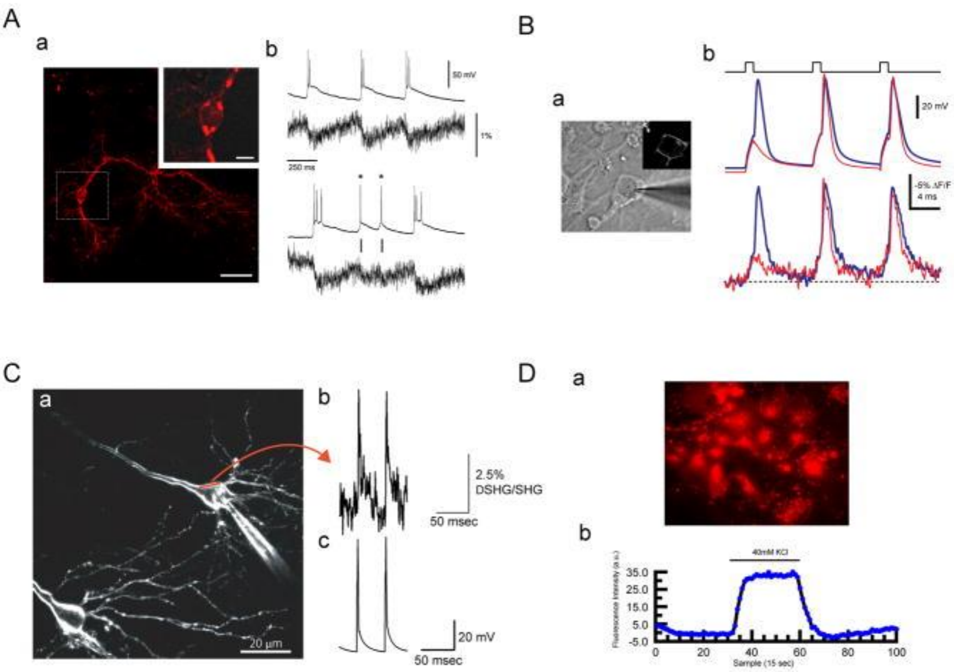

Figure 4.3: Voltage imaging in neurons [17].

4.1.2 Data collection by 10-20 mechanism

The OpenBCI cyton board is capable of reading the voltage variations resulting from the ionic charge within a period of time. The neural oscillations are recorded from multiple electrodes placed on the scalp, just as traditional electroencephalography (EEG) does [46]. The impulses are continuously generated since the brain never stops functioning. Thus, the classification of these for a diversified range of thought processes needs to be analysed [18].

The Daisy module is used along with the Cyton board for obtaining multiple readings from the additional electrode channels. This ensures the accuracy of the obtained data. The electrodes are placed all over the scalp region while maintaining according to the internationally acknowledged 10-20 system [39]. The 10-20 system implements in context to the original electroencephalography (EEG) practice. The arrangement has been developed to assure uniformity and conformity. Thus it allows the identification and correlation with a set of data [46]. The 10-20 system depends on the positioning of the electrodes that collect readings from the cerebral cortex. It is based on the periods of gaps that separate the adjoining electrodes. Hence, the 10-20 instructs administering the electrodes either 10% or 20% of the total front-back or right-left distance of the skull [46].

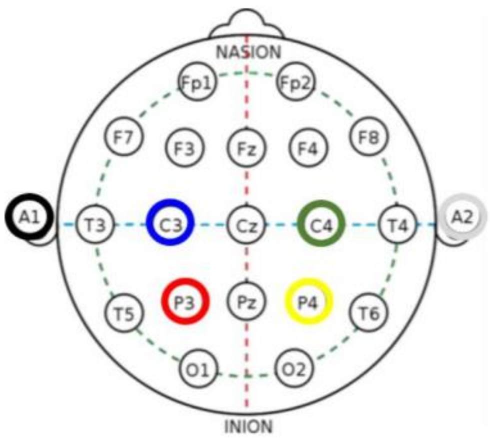

Figure 4.4: Electrode placement by 10-20 system [39].

4.2 Data analysis

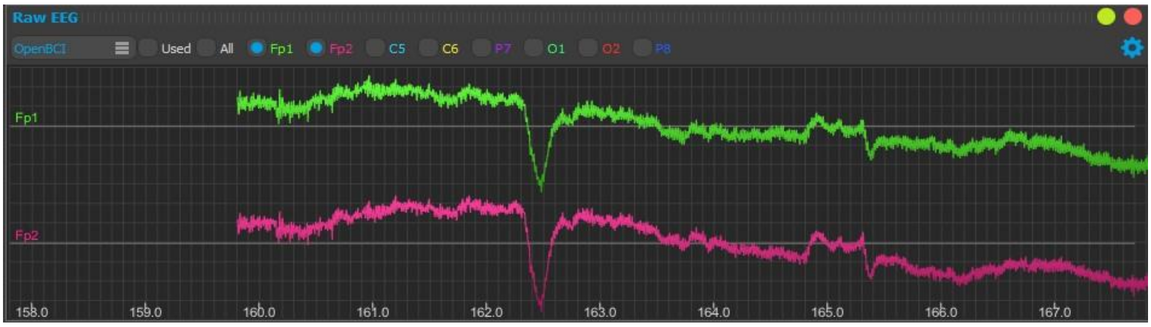

Figure 4.5: Raw data observation.

The data is initially observed in graphical construction with the help of the OpenBCI software. Originally, it displays a clustered form of the graph affected by the noise and interference involved [as illustrated in figure 4.5]. Noise appears in the system due to numerous determinants related to the position of the system and can often lead to unexpected outcomes [62]. However, many studies recommend the invasive technique over the non-invasive ones because of the better extraction of the signal properties. It is believed that the signal would be 20-100 times stronger when the EEG data is directly extracted from the interiors of the cortex [47]. The verdicts of the non-invasive EEG studies often advise to carefully reduce artefact noises (muscular movement) [63]. Neuroimaging the EEG signals during muscular movement can therefore be challenging to analyse. Since the EEG sensor signals are composites of active signal noises producing a low signal-to-noise ratio [49].

In most instances, we are surrounded by electronic devices and electrical appliances that are invariably transmitting signals. In a practical environment, the presence of electrical noises to some extent is unavoidable and such signals incorporate to the noises. The nearby devices that emit radiowaves frequently contribute to the noises. Similarly, electrical apparatus that produce magnetic fields such as motors, generators and so on, can also contribute to inconstancies of the signals [62]. Moreover, the internal circuitry of the OpenBCI equipment additionally produces trivial electrical noises. But it can make a significant impact when incorporated with the noises produced from long cables that connect the electrodes to the Cyton board. Thus the signal processing methods require improvements to enhance the classification performance [49].

4.3 Noise reduction method

Signal-to-noise ratio (SNR):

In the brain-computer interface (BCI) system, whole-brain signal-to-noise ratio (SNR) increases when being controlled in contrast to when not being controlled. Likewise, network-based classification of the observed EEG data supports that whole-brain SNR is usually high while performing tasks [50]. Among the collective methods of noise reduction to improve signal quality, the SNR performs an essential purpose. The signal-to-noise ratio (SNR) measures the power of the desired signal with respect to the power of the consolidated background noises and variances [61].

Regardless of whether the system is wired or wireless, SNR can directly influence the performance of the system. Higher noise accumulation would result in lower SNR and would eventually impede the network performance. Whereas, a higher value of SNR represents a stronger network and ensure a better throughput [57]. For instance, proclaimed results confirm that high accuracy can occur uniformly during low SNR [50]. The signal-to-noise ratio (SNR) computation is regarded as the conventional method of determining the reliability of brainwave activities. To ensure the prosperous transmission of valuable neural information, the electrodes implemented are made of metallic conductors such as gold. This ensures the accuracy of the obtained brainwave signals and enables further quantification and modification [61].

The obtained brainwave signal can be considered as the sum of the desired signal, s(t). Whereas, the noise signal and interferneces can be denoted as n(t). The overall signal can be represented in time-domain (t) as well as frequency domain (f) [54]:

$$x(t) = s(t) + n(t)$$

Upon reciveing the data, the signal-to-noise ratio (SNR) can be denoted in the frequency-domain [61]:

$$SNR = \frac{P(signal)}{P(noise)} = \frac{S(f)}{N(f)}$$

Where, the S(f) is the power density of the desired signal and the N(f) is the power density of the noise signal, both computed in frequency-domain [61].

However, signals are often expressed in logarithmic decibel scale (dB) [57]:

- $\Rightarrow$ $SNR_{dB} = 10\log_{10}$ (SNR)
- $\Rightarrow$ $SNR_{dB} = 10\log_{10} \left[\frac{P(signal)}{P(noise)} \right]$
- $\Rightarrow$ $SNR_{dB} = 10\log_{10}$ [$P_{(signal),dB}$ - $P_{(noise),dB}$]
- $\Rightarrow$ $SNR_{dB} = 10\log_{10} . P_{(signal),dB} - 10\log_{10} . P_{(noise),dB}$
- $\Rightarrow$ $SNR_{dB} = P_{(signal),dB} - P_{(noise),dB}$

4.4 Signal Filtering

4.4.1 Band pass filters:

Band Pass Filters (BPF) is a resistor-inductor-capacitor (RLC) circuit. BPF is created by cascading a low-pass filter (LPF) circuit with a high-pass filter (HPF) circuit. Thus, the developed filter, only allows frequencies within a specific band or range to pass. The cut-off frequency or fc of a specific bandwidth controls the successful passage of the allowed frequency ranges [68]. The band-pass filter plays a major role in the wireless communication industry. The BPF filters the transmitted signals according to the specific bandwidth between two specified frequency cut-off points, fc. The concept of fc is widely used in the WLAN network, audio amplifier circuits and high-speed wireless broadband, etcetera [69].

Bandwidth is commonly defined as the frequency range that exists between two specified frequency cut-off points (fc). The cut-off points are generally 3dB below the maximum amplitude. The bandwidth had a lower cut-off frequency (f_L) and a higher cut-off frequency (f_H). To ensure the functionality of the pass-band, the f_L must be higher than f_H [68].

Condition for BPF: $f_H > f_L$

$\Rightarrow$ BW = $f_H - f_L$

Computaion of the cut-off frequency (fc) [68]:

$$f_c = \frac{1}{2\pi RC}$$

The BPF has been utilised in our project for the desired range of brainwave frequency accumulation. To further screen out the signals outside the aspired range. Besides, attenuation or reduction of the signal is further ensured by the Butterworth filter characteristics. The attenuation of ripples in the pass-band and zero roll-off response in the stop-band delivers a smoother signal [76].

Generally, the Butterworth band-pass filter is designed using both IIR and FIR filters. The IIR filters produce non-linear phase or impulse response of infinite interval/duration. Whereas, the

FIR provides linear phase or impulse response of finite value [76]. Hence, the Butterworth BPF processes in bi-direction to provide the frequency response as flat as possible. It has a cut-off frequency (fc) ranging from 0.5 Hz to 60 Hz [72]. Thus it has a wide range of applications in the BCI system involving the EEG brainwaves signals. It can be implemented for regulating the band-pass filters for respective ranges of a brainwave. Reckoning, it can extract the distinct ranges of brainwaves such as Alpha, Beta, Gamma, Theta and Delta [72]. Therefore, when the band-pass filter is ranged between 0.5 Hz and 3 Hz, it is called the Delta frequency band-pass filter. Similarly, the band-pass filter with frequency varying between 4 Hz and 7 Hz is designated the Theta frequency band-pass filter. The Alpha frequency band-pass filter would, however, have a pass-band frequency of 8 Hz and band-stop frequency of 12 Hz. Likewise, a band-pass filter with a pass-band frequency of 13 Hz and band-stop frequency of 30 Hz would operate during the Beta frequency range. Lastly, any frequency ranging over 30 Hz would serve for the Gamma frequency band-pass filter [72]. The categorized brainwave ranges assigned to individual pass-bands can be advantageous for control and cognitive-based implementations. Furthermore, the growing technology market especially the field of telecommunication expects the further development of new applications in wireless communication [69].

Generalised equation of frequency response of n-th order Butterworth band-pass filter [76]:

$$H(j\omega) = \frac{1}{\sqrt{1 + {H_0}^2 \, [\frac{\omega}{\omega_c}]^{2n}}}$$

Where, n is the order of the band-pass filter and, $\omega = \frac{1}{f}$

$\Rightarrow \omega_c = \frac{1}{f_c}$

H_0 is the maximum pass-band gain, commonly defined at a frequency equal to the cut-off frequency.

H_0 can be represented in logarithmic-scale (in decibels) [76]:

1 dB = 20 log H_0

Moreover, the frequency response of the filter can be mathematically defined by its voltage transfer function [76]:

$$H(j\omega) = \frac{V_{out}\ (j\omega)}{V_{in}\ (j\omega)}$$

Where,

- ⇒ V_{out} is the output signal voltage.
- ⇒ V_{in} is the input signal voltage.
- ⇒ $\omega = \frac{1}{f}$

4.4.2 Notch filters:

A notch filter is also known as a band-stop filter or band-reject filter. These filters are designed to attenuate or cancel out signals at a specified frequency range [70]. The filter, therefore, allows all other frequencies to pass except for the selected frequencies.

The notch filter is composed of low-pass and high-pass filters. Unlike the cascading of the band-pass filter, the LPF and HPF in notch filter circuits are connected in parallel [71]. The LPF in a notch filter circuit passes the signals with frequencies lower than the higher cut-off frequency (f_H). On the other hand, the HPF of the notch filter circuit enables the passage of signals having frequencies higher than the lower cut-off frequency (f_L) [71].

As the name suggests, notch filters facilitate a notch or narrowband over which the filter eliminates the signals on that particular frequency. The block/drop in the region of frequency is displayed in the response plot. More often than not, notch filters are used for the expulsion of a fixed frequency [74]. The notch filter employed for EEG brainwave application precisely causes that. The pass-band covers four bands of brainwave and contributes to more than 65 dB attenuation for the 50 Hz power line interference [73]. These noises and interferences are generally present in our surroundings due to the presence of electrical and electronic devices. Hence, we can avoid signal corruption by excluding and refining the noise in the collected EEG brainwave signal and further improve the quality [73].

Notch filter frequency can be computed by [74]:

$$f_{notch} = \frac{1}{2\pi RC}$$

Where, C is the capacitance and R is the resistance of the circuit.

f_{notch} is the centre frequency that can be calculated as [68]:

$$f_{notch} = f_r = \sqrt{f_L \; f_H}$$

Where, f_H is the higher cut-off frequency and f_L is the lower cut-off frequency.

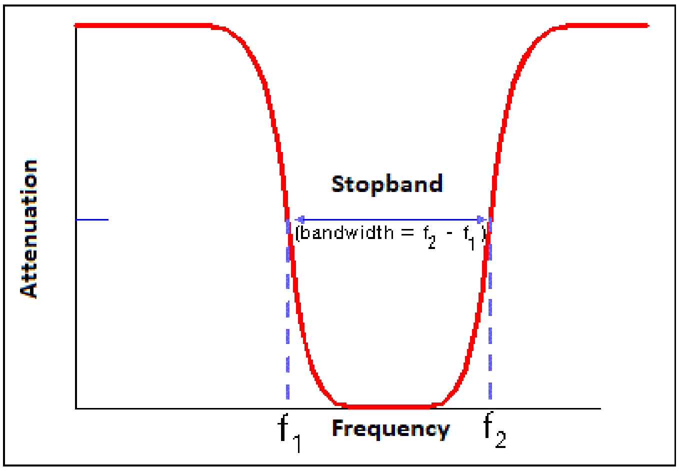

Figure 4.6: Frequency plot of a Notch filter [70].

4.5 Signal sampling theories

4.5.1 The Root Mean Square (RMS)

The Root Mean Square (RMS) is used to estimate the signal strength. The RMS average is a mathematical classification of the magnitude of the fluctuating EEG signals. Researchers have conventionally represented the EEG signal analysis has been conventionally represented in the frequency-domain to apply Fourier transform (FFT). Consequently, the signals consist of positive and negative variations since they are sinusoidal signals. RMS is used in signal processing of various applications; it is generally defined by [65]:

$$\sqrt{\frac{\sum_{i=1}^{M} |X_i|^2}{M}}$$

Where, X_i is the i-th component of the signal $x(t)$ in the frequency-domain [65].

4.5.2 Fast Fourier Transform

The Fast Fourier Transform (FFT) has been used to obtain the electroencephalography (EEG) data to analyze the characteristics of the brainwave signals in the frequency-domain [20]. The FFT method enables computing the DFT in (nlogn) time. The basic idea of the FFT is to divide the coefficient vector of the polynomial into two vectors, recursively compute the DFT for each of them, and combine the results to compute the DFT of the comprehensive polynomial [54].

Generally, the time and frequency domains each contain one signal made up of n complex points. Each of these complex points is composed of two numbers, the real part and the imaginary part. The FFT functions by decomposing an n point time-domain signal into n frequency-domain signal, while they each have a singular point. Thereafter, the n frequency-domain spectra are calculated corresponding to the n time-domain signals. Lastly, n spectra are synthesized into a single frequency spectrum [64].

The derivations of the FFT equation in general form is expressed as [56] :

$$F\ (n) = \sum_{x=0}^{N-1} [\ f(\mathrm{x})\ .\ (e^{-\frac{j2\pi}{N}})^{n\,x}\ ]$$

Where, n have the integer value of complex points,

n = 0, 1, 2, 3,…., (N-1)

and $e^{-\frac{j2\pi}{N}}$ is a primitive of Nth root of one [56].

The collected EEG signals are segmented and equated according to functionality requirements. After that, the frequency spectrum using the mean EEG signal is determined using the fast Fourier transform (FFT) technique in OpenBCI GUI software. The observed spectrum is fixated and further utilised in BCI applications. However, the FFT spectrum cannot manipulate temporary data in MATLAB application and only displays the selected saved ones [55].

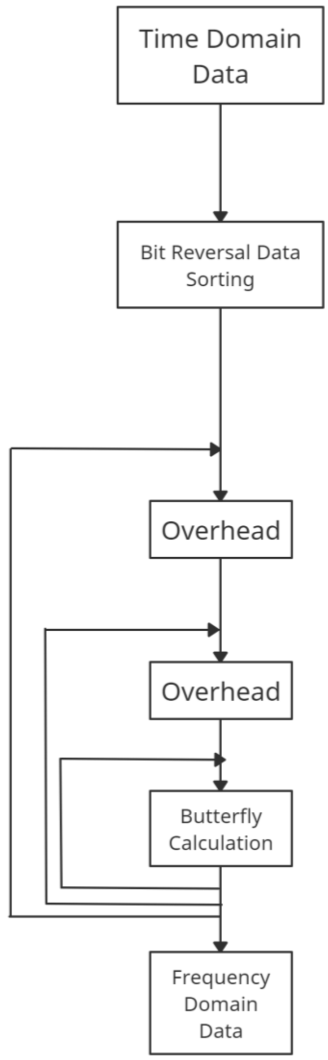

Figure 4.7: The fast Fourier transform (FFT) flow diagram.

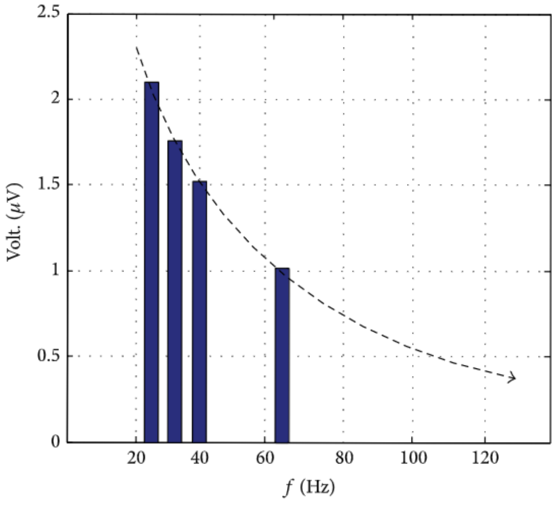

Figure 4.8: Example of a fitted curve of FFT [55].

4.5.3 Nyquist-Shannon sampling theory:

The Nyquist-Shannon theorem serves as the fundamental bridge between the continuous-time and the discrete-time signals. The theorem concedes adequate condition for the sample rate that is required for sampling. This enables the sampling of a discrete sequence from a bandwidth of continuous-time EEG signal, such as a sinusoidal frequency. However, the condition stated by the Nyquist theorem is to sample double of that of the original signal [66].

The Nyquist theorem characterises the sampling method of a signal/waveform without losing the intrinsic information. For instance, a signal x(t) within a bandwidth would have frequency limits. Upon the application of Fourier transform on x(t) signal, a maximum frequency of fmax would be acquired. Therefore, beyond the maximum frequency limit, fmax, the signal would not generate any energy. Thus the Nyquist theorem suggests that: to sample the signal x(t), we would need to sample the signal with a frequency larger than twice its maximum frequency, f_{max} [59]:

$$\Rightarrow f_{sample} \geq 2\, f_{max}$$

$$\Rightarrow f_{Nyquist} = \frac{1}{2}\, f_{sample}$$

Similarly, the Nyquist theorem can be stated in context to the time period [59]:

$$\Delta t_{sample} \leq \frac{1}{2} \Delta t_{min}$$

Where, $\Delta t_{min} = 1/f_{max}$

Δt_{min} is the time period during the maximum frequency [59].

The precise representation of the Nyquist-Shannon sampling theorem suggest that, in a continuous-time signal *x(t)* with Fourier transform *X(ω).*

Where, $X(\omega)$ is in the range of : $(-\pi /T) < \omega < (\pi /T)$, otherwise $X(\omega) = 0$.

Upon Fourier transform of the signal x(t), we achieve X(ω) [67]:

$$x(t) = \frac{1}{2\pi}\int_{-\infty}^{\infty} X(\omega)e^{j\omega t}\, d\omega$$

Considering no frequency component higher than π/T [67]:

$$x(t) = \frac{1}{2\pi}\int_{-\pi/T}^{\pi/T} X(\omega)e^{j\omega t}\, d\omega$$

Sampling the signal with T interval, sampling is linear (not time invariant) [67]:

$$y(n) = x(nT)$$

$$y(n) = \frac{1}{2\pi}\int_{-\pi/T}^{\pi/T} X(\omega)\, e^{j\omega nT}\ d\omega$$

Changing the variable [$\boldsymbol{\omega T = \theta}$], then further comparing the expression for the inverse discrete-time Fourier transform (DTFT) [67]:

$$\Rightarrow\ y(n) = \frac{1}{2\pi\, T}\int_{-\infty}^{\infty} X(\frac{\theta}{T})\, e^{j\theta n}\ d\theta$$

$$\Rightarrow\ y(n) = \frac{1}{2\pi}\int_{-\infty}^{\infty} Y(\theta)\, e^{j\theta n}\ d\theta$$

Hence, in the range: [$-\pi < \theta < \pi$], Y has the same shape as X although it has been scaled. Since Y is periodic with a periodicity of 360° = 2π, thus if Y is known in the abovementioned range of frequencies then it can be known for all frequesncies. It can be written as [67]:

$$\Rightarrow\ Y(\theta) = \frac{1}{T}\ X(\frac{\theta}{T})$$

$$\Rightarrow\ Y(\theta) = \frac{1}{T}\sum_{k=-\infty}^{\infty} X\left(\frac{\theta - 2\pi k}{T}\right)$$

Therefore, Shannon's channel capacity for each of the channels [58]:

$$\Rightarrow\ C = \log\frac{\beta+2}{\beta}$$

$$\Rightarrow\ C = B\ log_2\ (1 + SNR)$$

Where, C is the capacity of the noise channel, SNR is the signal-to-noise ratio and B is the bandwidth of the channel [58].

4.6 Signal transmission

4.6.1 Serial communication

The networking widget in the OpenBCI portal enables the streaming of data. This can be further implemented into applications and software. For instance, by employing serial communication we can stream one data type. The data is transmitted bit by bit in the form of continuous packets. The transmission of the data is maintained sequentially to facilitate successful interface with microcontrollers. Hence, this concedes logical networking protocols that can be applied when using OpenBCI with Arduino [75].

Serial communication between the OpenBCI and Arduino maintains a baud rate. It is the rate at which the data is being transferred in bits per second. The baud rate of the receiving application must correspond to that chosen by the sender. Moreover, serial communication further emphasizes on assigning the ports of the receiver that are being utilised. For instance, in the case of Adruino, the port assigned is generally "USB modem" which has a serial number attached to it [75].

4.6.2 Lab Streaming Layer

The Lab Streaming Layer (LSL) is yet another networking system in the OpenBCI applications. It is a method used for synchronizing the collected data that is being streamed into the system. This permits the data to be recorded for future usage and analysis. LSL is a beneficial technique to transmit the OpenBCI stream into applications for further manipulation of the data. Applications such as MATLAB, Python and so on are useful tools for handling EEG readings [77].

The fast Fourier transform (FFT) used for data extraction and acquisition, is an efficient tool if computed favourably. The FFT involves wide ranges of mathematical advancements. It comprises simple and complex numbers resulting in NlogN operations, where N is the length of vector ranging in thousands/millions. Accordingly, manual techniques wouldn't possibly generate productive outcomes [72]. The computational analysis would be far more efficient and accurate for the transformation of domains (time-to-frequency) of the signals. The fast Fourier transform (FFT) data can also be transmitted through the lab streaming layer (LSL) [77].

Chapter 5

Result and Analysis

This chapter discusses the overall outcomes of our project thus far. As per our project comprehension in the previous chapters, the intention is to correlate the theory to the computational analysis and applications.

5.1 Work Methodology

As discussed earlier, the primary objective of our project outline is data acquisition from the brain. Figure 5.1 illustrates the concept of the manifested initial stages of our work. We have collected the brainwave signals by placing electrode-caps to the surface of the scalp. The conductive paste has enhanced the transmission of the data signals. Cyton-biosensing board has enabled the accumulation of the signals that we have later visualised with the help of OpenBCI GUI application. The GUI has permitted the observation of the filtered and transformed data in real-time, as we continued transmission. Furthermore, the apparent data signals have been recorded in .txt format for future implementations. The networking techniques of lab streaming layer (LSL) and serial communication, as described in chapter 4, has enabled us to transmit the data for various purposes. We have administered subjective outcomes by applying these networking protocols.

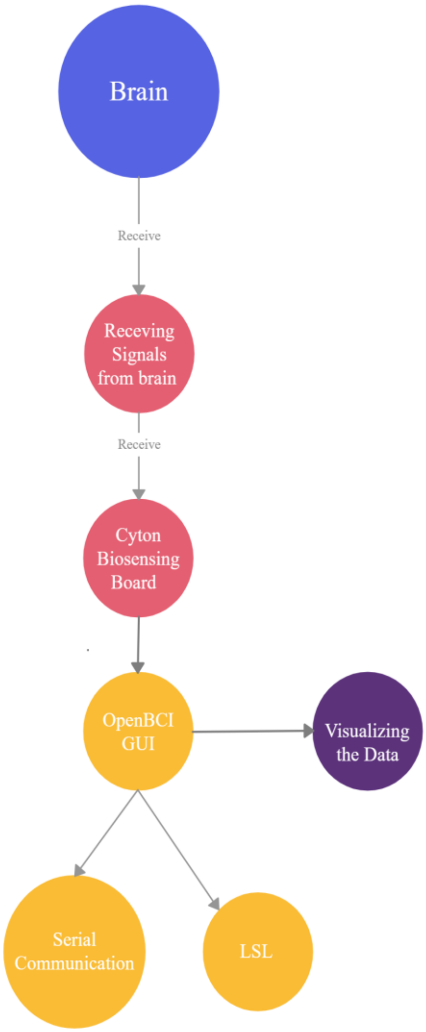

Figure 5.1: Concept map of the initial stages.

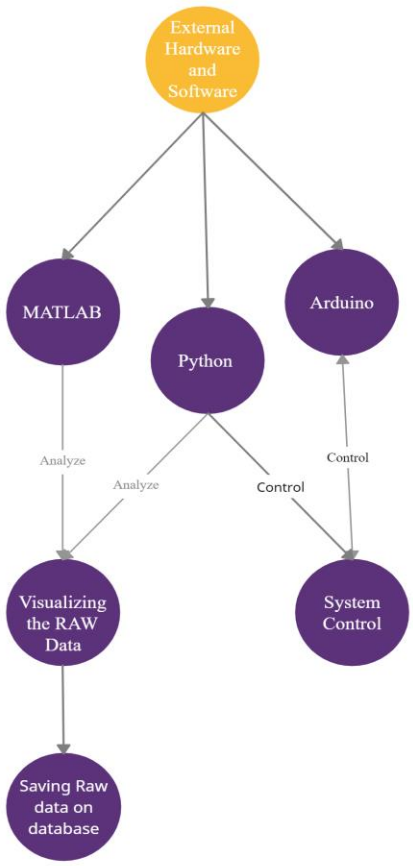

Figure 5.2: Analysis of the acquired data.

In above figure 5.2, it is described how we have consolidated our accumulated data for further utilisation. In an instance of broadcasting the data to a software system, we have used the lab streaming layer (LSL) networking protocol. This has allowed us to transfer data into Python and MATLAB. We have used the MATLAB application to observe the graphical plots of the unfiltered raw data that we have assembled. The collected data has also been saved in our database for future applications.

Moreover, we have utilised the collected data through serial communication with a microcontroller such as Arduino. This has allowed us to execute the control-based application that we had anticipated.

Figure 5.3 illustrated below, demonstrates the types of system control that we have been able to accomplish. The home automation has been achieved by the restriction of LED flickering using the brainwave signals. We have also gained control of basic computer administration, such as scrolling through the feed or window in applications. Most importantly, we were able to control the motion of a robotic car with brainwave signals alone.

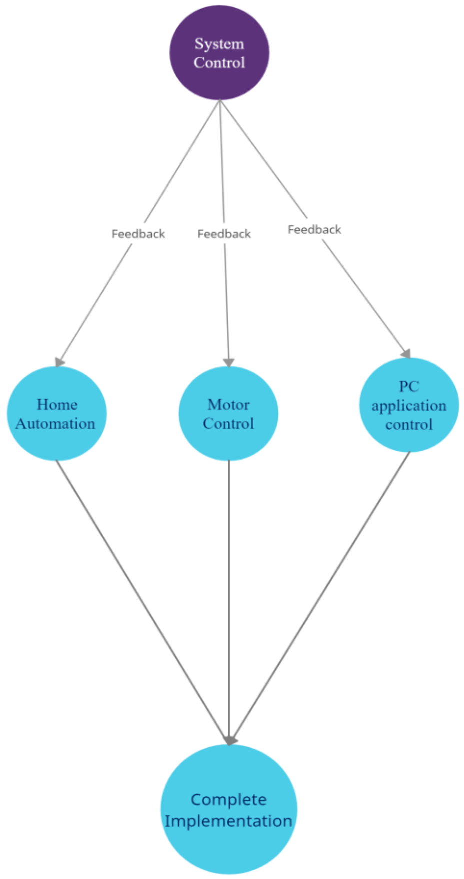

Figure 5.3: Implementation of the data.

5.2 Data observation

The observation of the EEG brainwave readings on the OpenBCI GUI application has been provided in this section. The observable figures display the following information regarding the brainwave signals:

- Vrms plots (RMS vs. Time): measures the impedance of the brain signals in continuous-time period, which determines the signal strength. The graphical plot of Vrms illustrates the original data in time-domain.
- FFT plots (Potential vs. Frequency): measures the frequency of the generated brainwave signal along with the action potential (in micro volts). The graph displays the signal activity after filtering and FFT (to convert to the frequency-domain) has been applied. FFT makes the brainwave readable and easier, this helps to determine the brainwave classification range (i.e. Alpha, Beta, Theta, etc.). Generally, the action potential in the conscious state of mind shows readings in the range of 0.5 μV to 10 μV (micro volts).
- Head activity region: illustrates the active region in the brain at the instant of individual case. As per our discussion in chapter 2, the brain displays activity constantly at all instances. Thefore, for specific unbiased observations for clarification of the study of the region, we have used active channels in that region only (in cases that are mention). In all other cases, all of the channels connecting to the Cython board, has been active to provide multiple readings for better understanding.

5.2.1 Observation during visual functioning

Case 1: Eyes closed

Initially, we have plotted and observed the output data of the brainwave signals that are generated when the eyes are closed. In the following case, the subject was awake and in conscious state. When the eyes were shut and the subject was in a relaxed stated, we have observed the following graphs in figure 5.4 and figure 5.5. There are little to no spikes in the graphs as the frontal lobe channels were avoided for precise reading of the eye movement.

Figure 5.4: Vrms plot when eyes are closed.

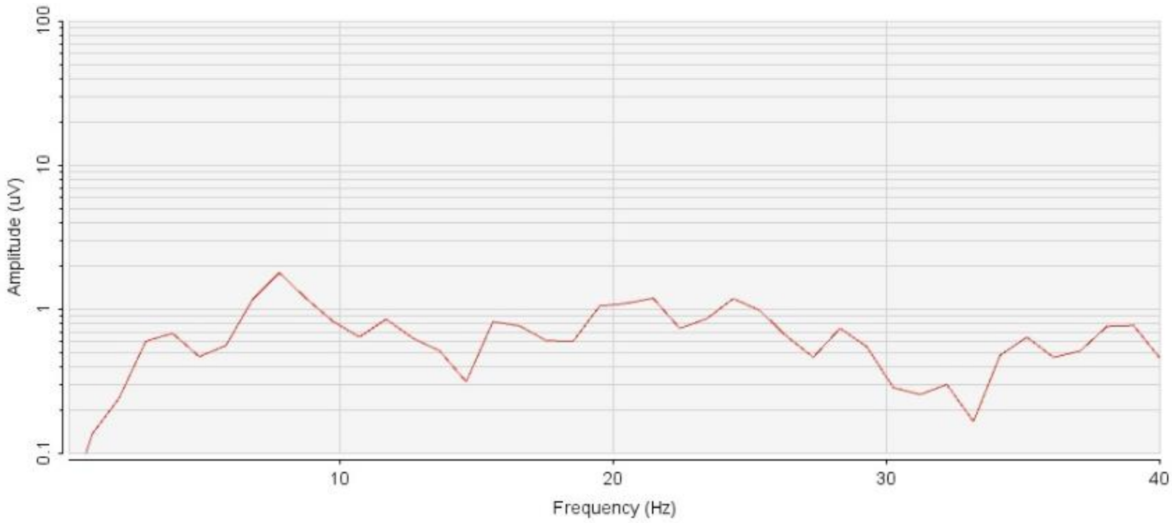

Figure 5.5: FFT plot when eyes are closed.

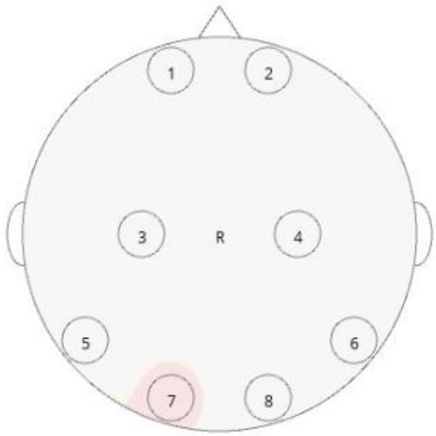

Figure 5.6: Head activity region when eyes are closed.

As we can see in the above diagram, the temporal region shows almost little to no activity due to the relaxation state of the subject. Considering the subject is in a state of Alpha brainwave frequency, the active frequencies can be observed in the FFT plot to be around 8-9.5 Hz. The activity of the occipital lobe is highlighted by channel 7 in figure 5.4. This suggests that visual processing is active, however, the subjects' eyes were kept closed.

Case 2: Eyes blinked once

Figure 5.7: Vrms plot when eyes blinked once.

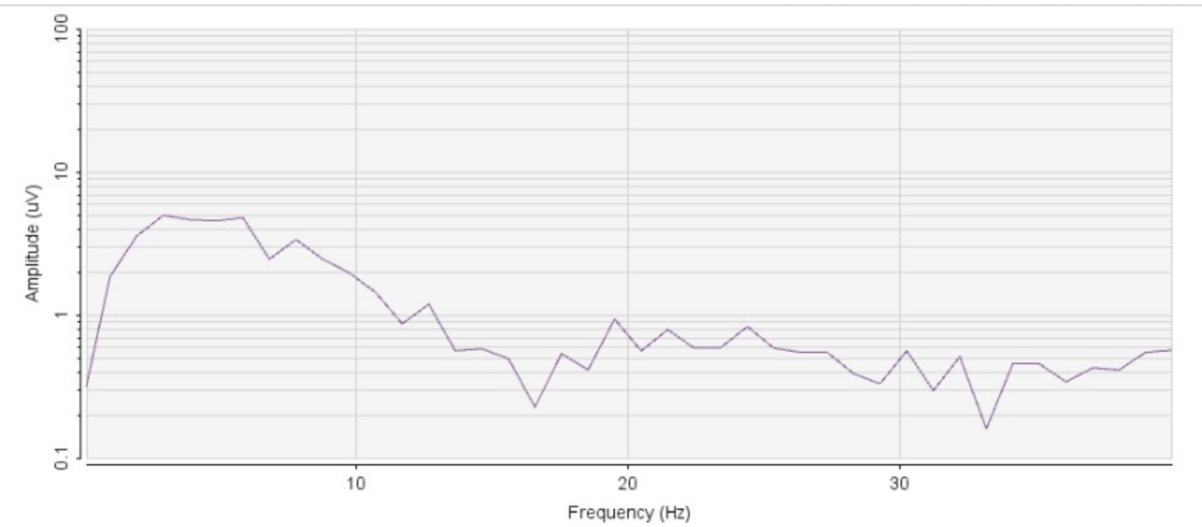

Figure 5.8: FFT plot when eyes blinked once.

Figure 5.7 shows a clear spike once, suggesting that the subject's brain activity changed in one instance. Here, the subject was asked to blink only once. In the FFT plot of figure 5.8, the frequency activity ranges below 10 Hz. This implies that the subject is still in Alpha brainwave rhythms and a state of calmness yet consciousness. The head region activity further indicates the activity in channel 2, suggesting the spikes generated in the frontal lobe of the brain region.

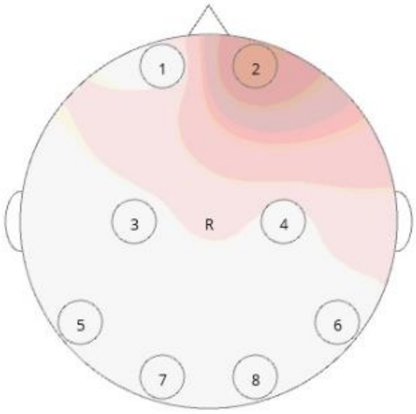

Figure 5.9: Head region activity when eyes blinked once.

Case 3: Continuous eye blinking

The following plots illustrate the data during continuous blinking of the eyes in a steady state condition of the body. The multiple spikes indicate the eyes' motion only while sitting down for the continuous-time period. However, according to the FFT plot, it is evident that the focus of the subject has developed. Since, the frequency activity is now further assumed nearing the range of Beta wave, i.e. around 12 Hz. The state is belived to read both Alpha and Beta brainwaves actively.

Figure 5.10: Vrms plot for continuous eye blinking.

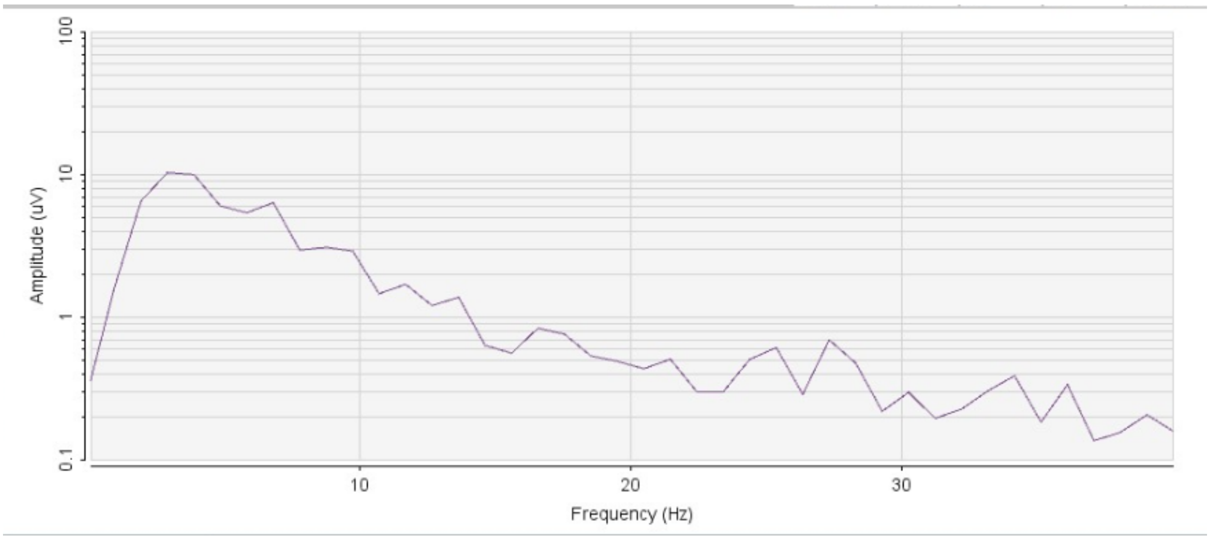

Figure 5.11: FFT plot for continuous eye blinking.

5.2.2 Observation during rest and motion

Case 1: During relax state

Figure 5.12: Vrms plot during relax state.

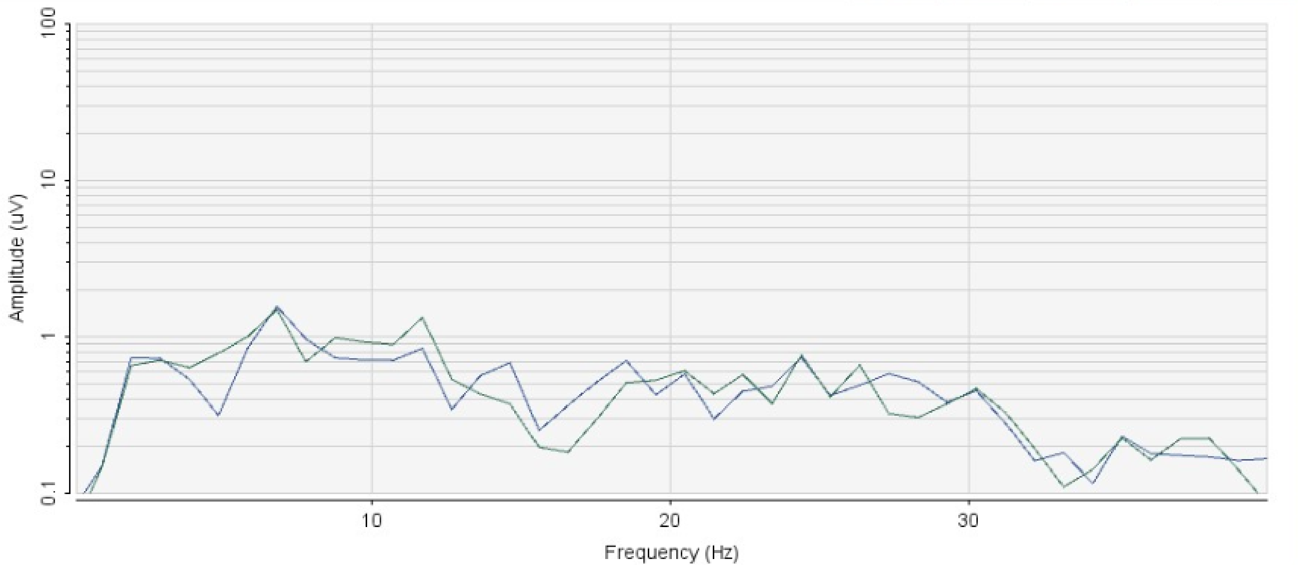

Figure 5.13: FFT plot during relax state.

As we can see in figure 5.12 and 5.13, the reading are quite steady during relax state. When the subject was almost asleep, the fluctuation dropped significantly nearing the Theta region with higher activity below 8 Hz frequency. Moreover, the action potential is significantly lower. Figure 5.14 further supports the trivial activity of the brain, the frontal lobe is generally inactive at this state of the body.

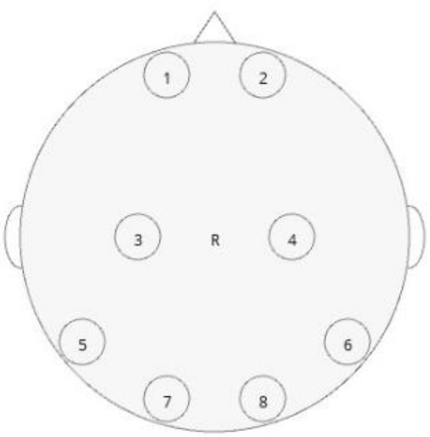

Figure 5.14: Head region plot during relax state.

Case 2: While walking

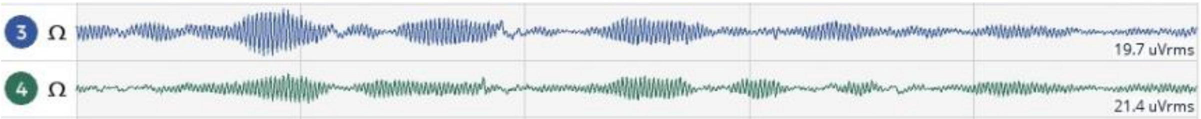

Figure 5.15: Vrms plot while walking.

The readings for motor activity significantly increases the brainwave functions as observed in figure 5.15 and 5.16. The muscular movements (artefacts) activates the parietal lobes along with the frontal lobes. This clearly increases the frequency and consciousness than when the subject was in rest. It can be implied that now the brain activity also involves Beta wave features.

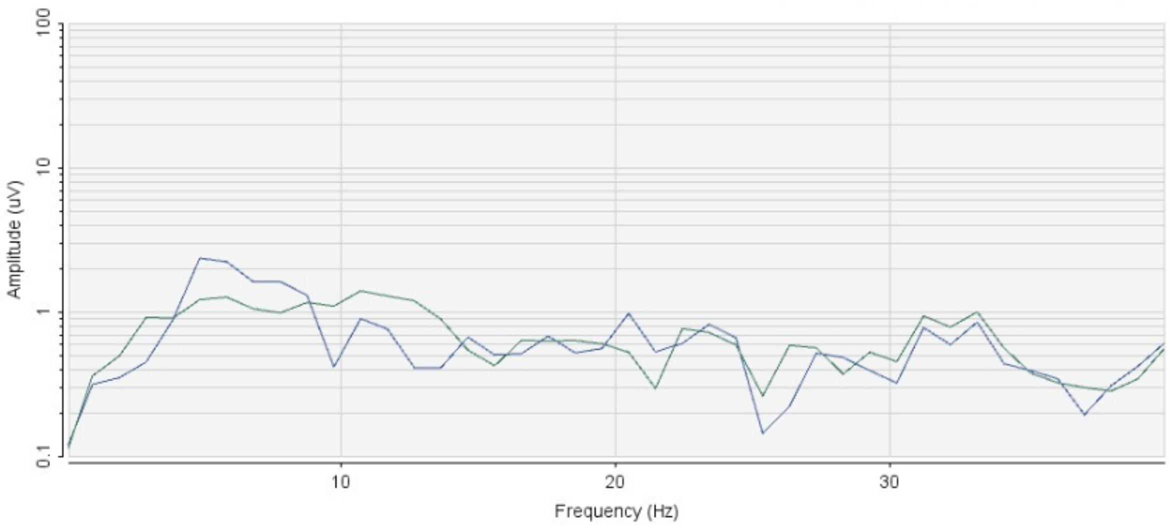

Figure 5.16: FFT plot while walking.

Furthermore, figure 5.17 indicates higher activity in the motor functions of the brain. It can be observed that channel 3 and 4 show significant movement.

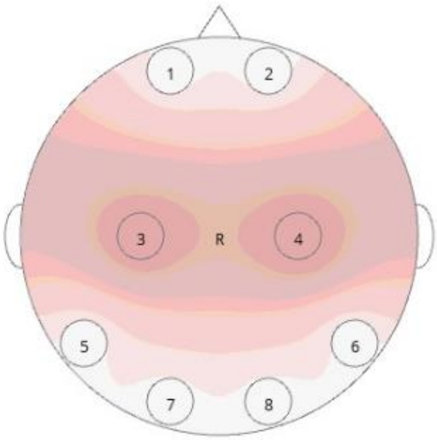

Figure 5.17: Head region plot while walking.

Case 3: While walking and arm movement

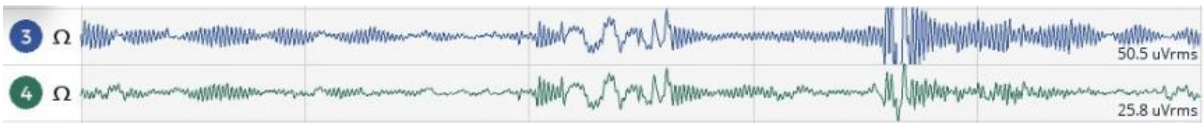

Figure 5.18: Vrms plot for walking and arm movement.

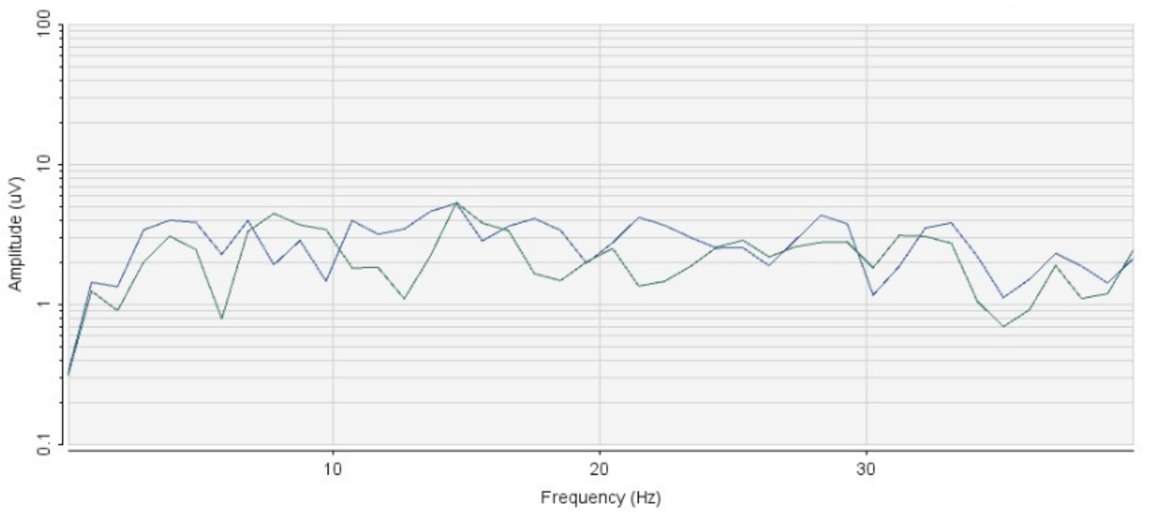

Figure 5.19: FFT plot for walking and arm movement.

For walking and arm movement, the fluctuations have further increased in comparison to the previous case. Figure 5.18 and 5.19 visualizes wider fluctuations and higher frequency ranges. This indicates the higher motor function of the body, as the channels 3 and 4 have higher activity than before as illustrated in figure 5.20.

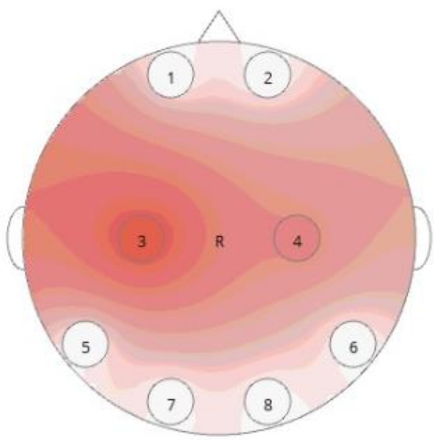

Figure 5.20: Head activity region plot for walking and arm movement.

5.2.3 Observation for cognitive functioning

Case 1: During reading and thinking

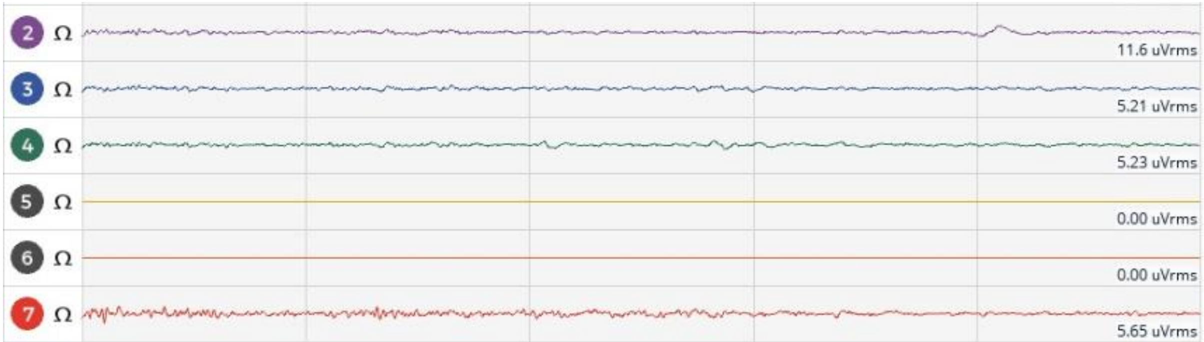

Figure 5.21: Vrms plot during reading and thinking.

During reading and critical thinking, while sitting down, we have observed brainwave readings in several regions. Figure 5.21 and 5.22 shows the multiple brain activities with a slightly higher action potential in contrast to the previous cases.

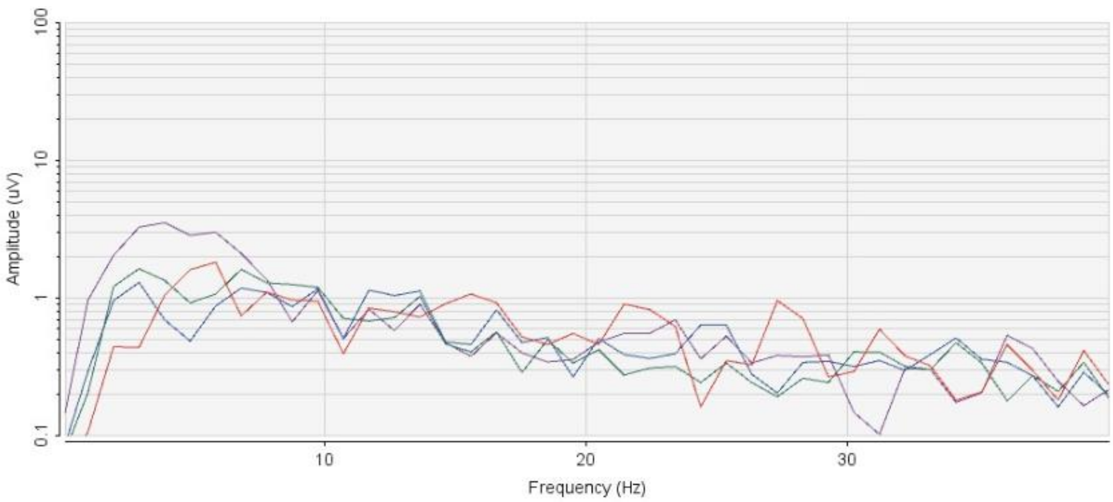

Figure 5.22: FFT plot during reading and thinking.

As observed in figure 5.23, channels 2 and 7 are highly active. This indicates the brain activity in frontal lobes suggesting that there is a high cognitive function and almost no motor function.

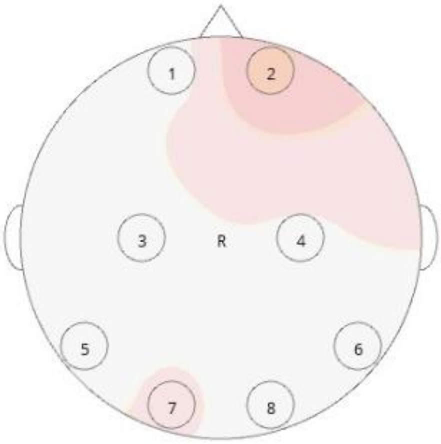

Figure 5.23: Head activity region plot during reading and thinking.

Case 2: During reading while moving

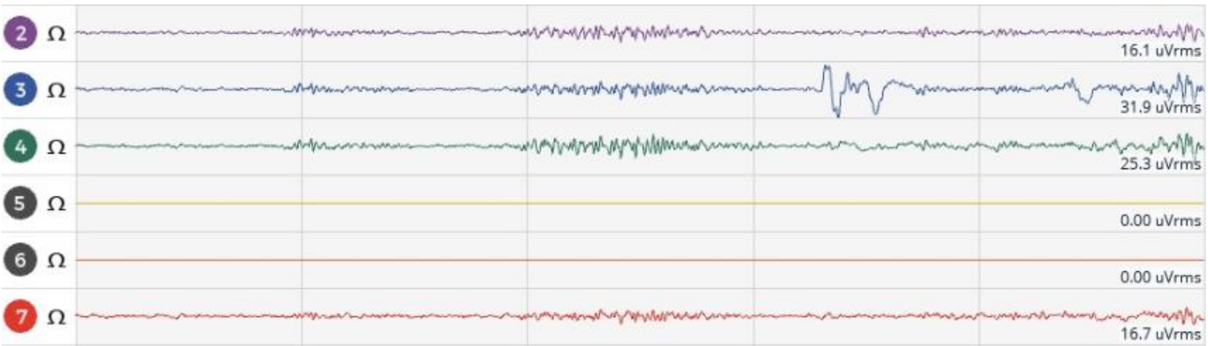

Figure 5.24: Vrms plot during reading while moving.

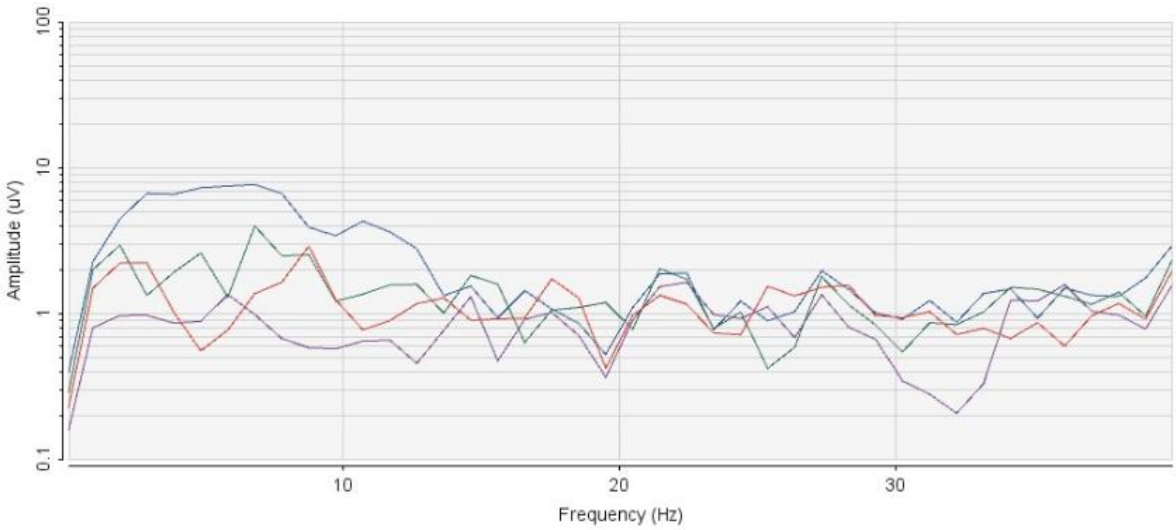

Figure 5.25: FFT plot during reading while moving.

The brainwave plots in figure 5.24 and 5.25 manifest the changes due to the increased movement. In this case, the subject was observed to read while walking. Hence, the active movement has added fluctuations to the preliminary existing ones. The frequency ranges in the higher Beta state along with the Alpha state. Action potential value has significantly increased as observed. Figure 5.26 further clarifies the instantaneous activity in the motor function region along with the cognitive function. The activity in channels 3 and 4 and distinctively increased and is higher the frontal lobe region as well.

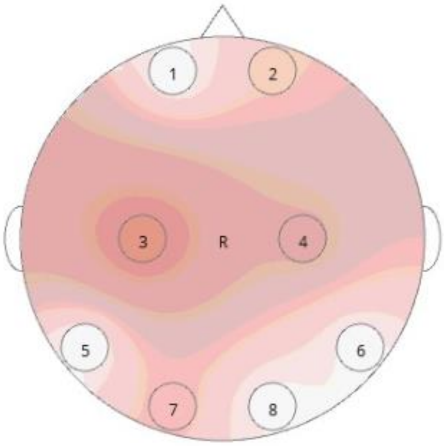

Figure 5.26: Head activity region plot during reading while moving.

Case 3: For reading while immobile

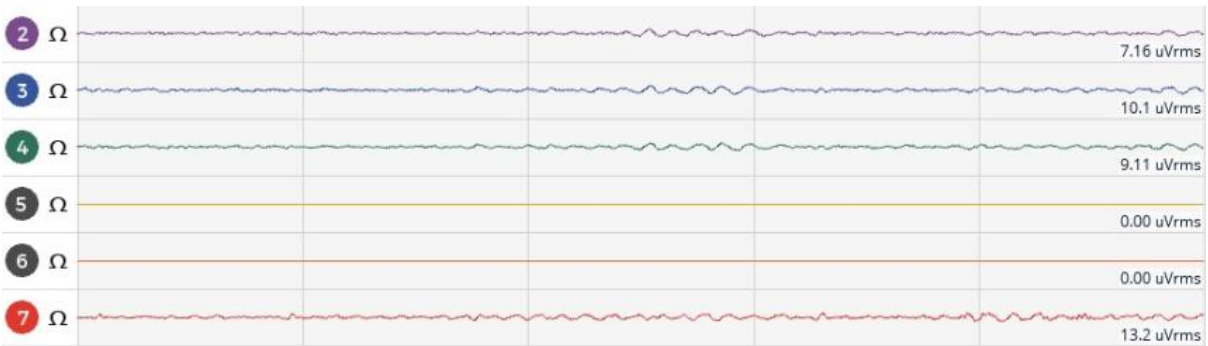

Figure 5.27: Vrms plot for reading while immobile.

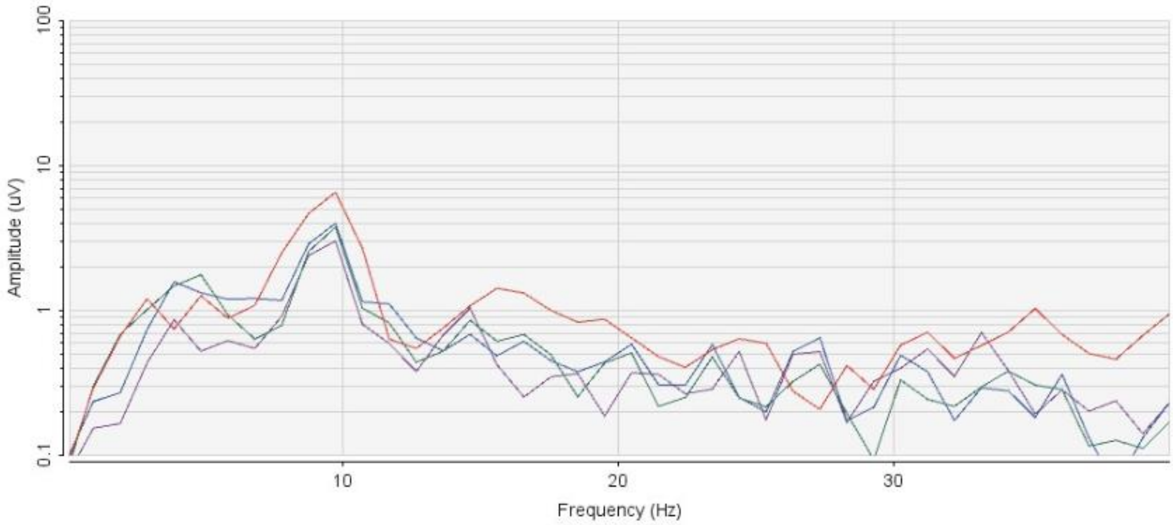

Figure 5.28: FFT plot for reading while immobile.

The activity of reading while in a resting state indicates that the cognitive functioning remains unchanged. As observed in figure 5.27 and 5.28, the brainwave frequencies are similar to that of the previous case. This suggests that the frequency range still exists in the higher Beta and Alpha range. Figure 5.29 shows activity in channel 7 only due to the immobility. Although the channels are connected for observation of motor functions, it is observably inactive since the subject is performing cognitive tasks while at rest.

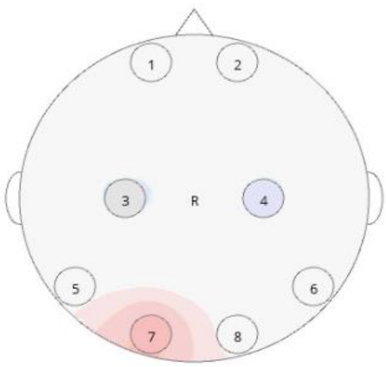

Figure 5.29: Head region activity for reading while immobile.

Case 4: For focus and concentration while immobile

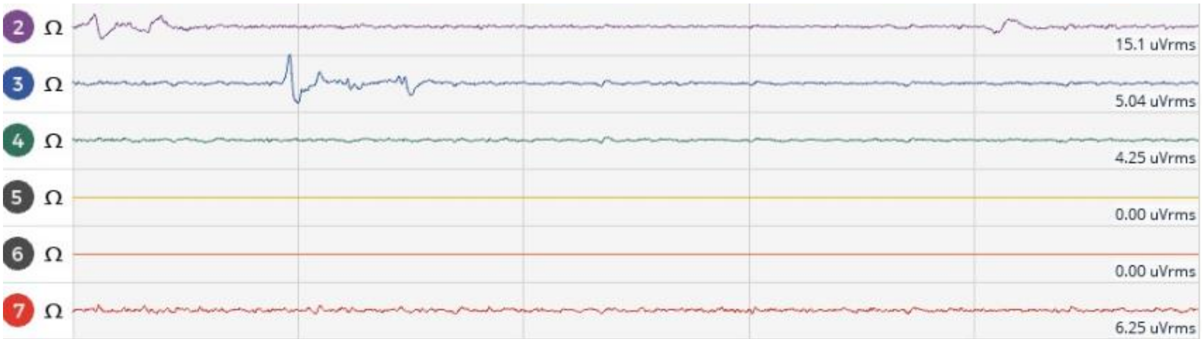

Figure 5.30: Vrms plot for focus and concentration while immobile.

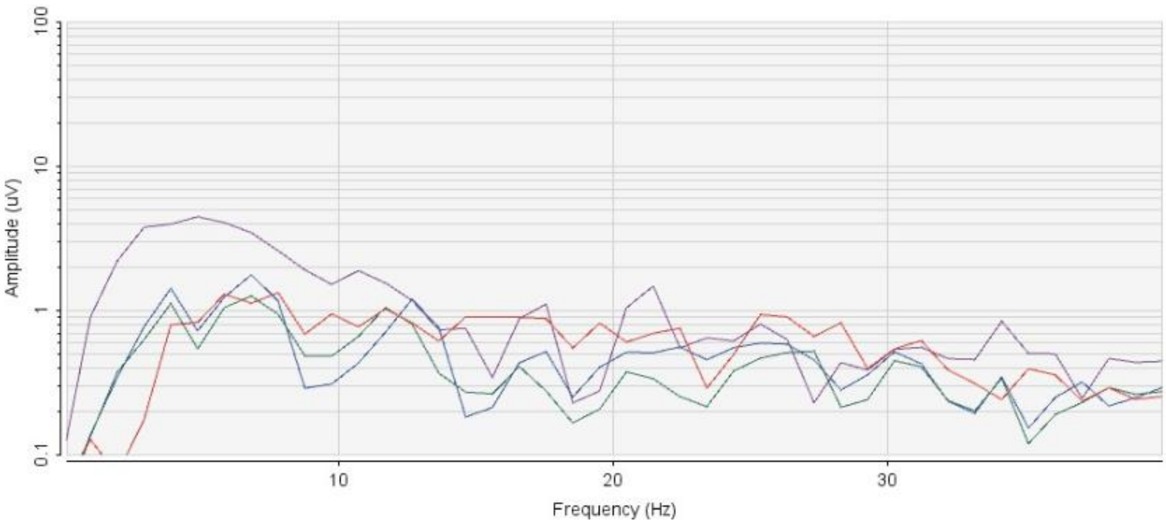

Figure 5.31: FFT plot for focus and concentration while immobile.

For focus and concentration, while immobile, the cognitive functions are seemingly consistent. However, due to the absence of mobility, the artefact (muscular movements) have significantly dropped indicating less motor function. Figure 5.30 and 5.31 apparently displays similar frequencies ranging between Alpha and Beta state as the previous case. Whereas figure 5.32

shows the cognitive functionality to be as consistent as anticipated, regardless of motor functionality. This can, therefore, be further implemented for control functions in the absence of movement.

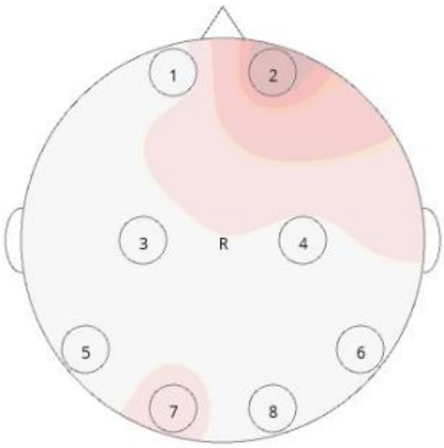

Figure 5.32: Head region activity plot for focus and concentration while immobile.

5.3 Data implementation and discussion

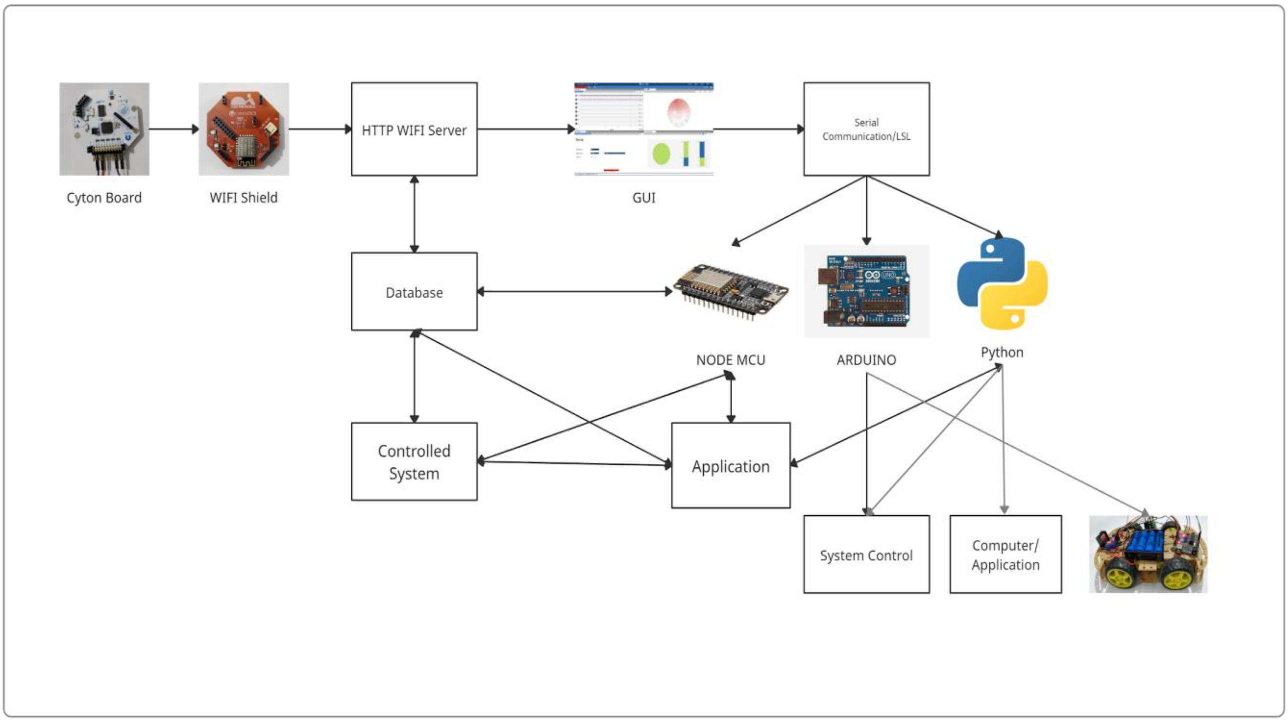

Figure 5.33: Block diagram overview of data analysis and implementation.

As discussed earlier in this chapter, the accumulation of brainwave reading is administered by the Cyton board and is further dispatched into diverse systems. The Wifi shield along with the help of HTTP WiFi server enables the transmission of the data. The transferred data is either sent to the OpenBCI GUI or saved in our database for future analysis and implementation (real-time).

The study of the data in the form of graphical output is visualised in the OpenBCI GUI. The GUI generally receives the data faster than a dongle, hence enables the observation and communication of the data in real-time. The data is further transmitted by networking through serial communication and/or lab streaming layer (LSL). We have conducted the networking protocols in affiliation to a microcontroller such as Arduino and the Python software for system control. Furthermore, the observation of the various cases in the previous section has been indispensable. Since, we have deduced that control-system can be enabled in the assigned ranges of brainwave frequency concerning focus and cognition. We have executed the control of a robotic car, LED light and computer scrolling. Further discussion of the implementation is in the next sections.

5.3.1 Focus control of a robotic car

System control with Arduino microcontroller has been accomplished by using the collected brainwave reading only. The brainwave data that have been collected and transmitted by the OpenBCI GUI has used the networking technique of serial communication for this purpose. Serial communication between the GUI and Arduino exhibits upon a particular baud rate for successful transmission. The port connection of the Arduino has been assigned for maintaining aligned network with GUI. We have baud rate specified at 57600 and the port assigned to COM4 as shown in figure 5.34. The Arduino-based robotic car has been tested on several occasions for motion control using the brainwaves signal data on a real-time basis.

The data of the brainwaves during the focus and concentration state has been utilized. The focus state of brainwave allows the general movement of the car. Upon losing the focus, the car stops moving. The focus state frequencies can be controlled by the control of the action potential threshold values. Since the principle of fast Fourier transform (FFT) depends on the inverse theorem of discrete-time Fourier transform (DTFT), the frequency-domain can be inversed in respect to time-domain that measures the impedance of brainwave activity. The threshold values of the impedance are set according to the observations of focus and concentration made in the earlier sections. The average human exercises the focus and cognitive functionalities in the brainwave ranges of Alpha and Beta, hence the impedance threshold is set as per each level [79]:

Beta frequency ranges from 13-32 Hz, which is observable in 0-0.7 μV (micro Volts) of brainwave impedance level.

Alpha frequency ranges between 8-12 Hz, which is detectable at impedance level of 0.7-2 μV (micro Volts) of brainwave signals.

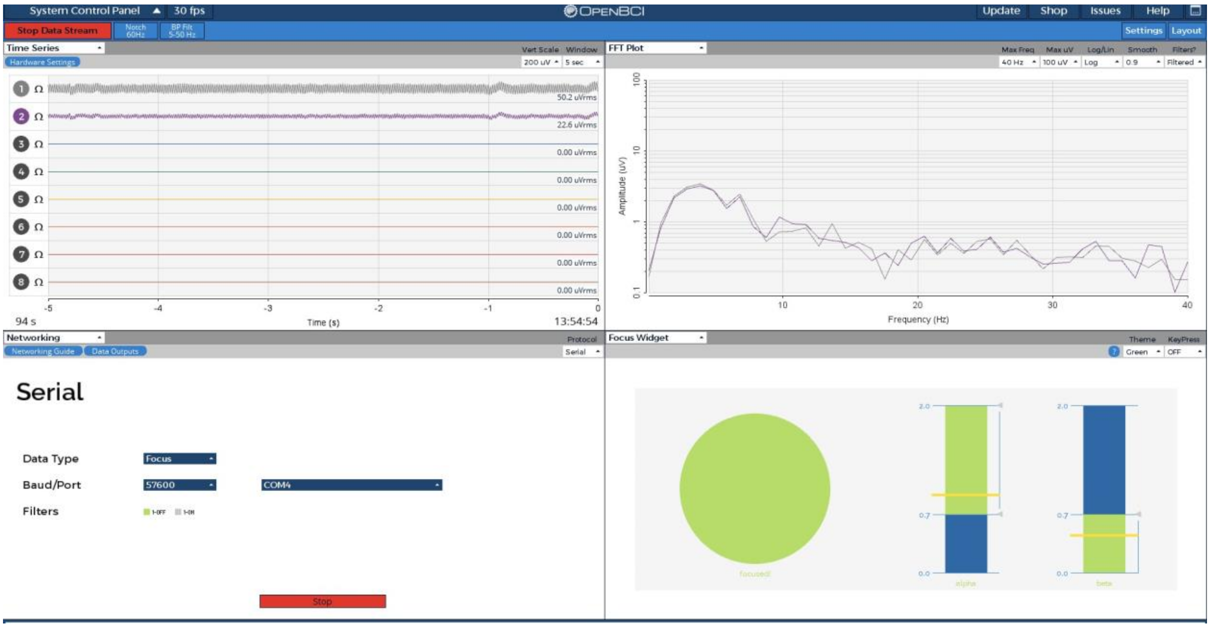

Figure 5.34: OpenBCI GUI plot for focus control of a robotic car.

The instant the focus state is activated, the car gains motion. The control over the focus state is challenging over a wide band of the burst of frequencies being constantly generated. Hence, we have implemented threshold values of the action potential/impedance according to the preferences mentioned above. The applied threshold values accommodate in the mapping of the heightened focus and control of the brain waves in this range which can be perceived in figure 5.34. The peaks at the Vrms plot indicate the entering of the focus state, which eventually initializes the motion of the robotic car. Figure 5.35 display the head region activity during the focus-based controlling state of the car at channel 2. The directional function of the car depends on the occipital lobe of the brain activating channel 7. It is responsible to administer the motor functions of the body as well.

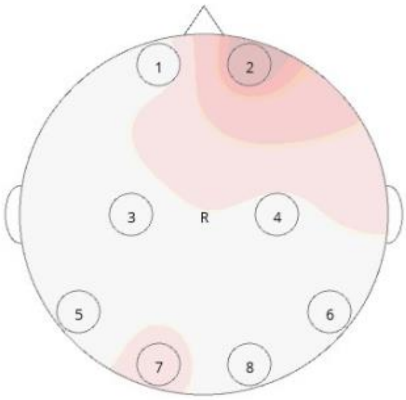

Figure 5.35: Head region activity plot for focus control of a robotic car.

Thus, when in the focus state, the car continuously keeps moving. However, the car stops operating the very moment that focus has been lost. When the subject is out of the impedance threshold values set for focus state, we observe peaks at the negative time values, as displayed in figure 5.36. The observed spikes in the negative time value axis, indicate the time delay. The time delay secures the retrieval of the focus state.

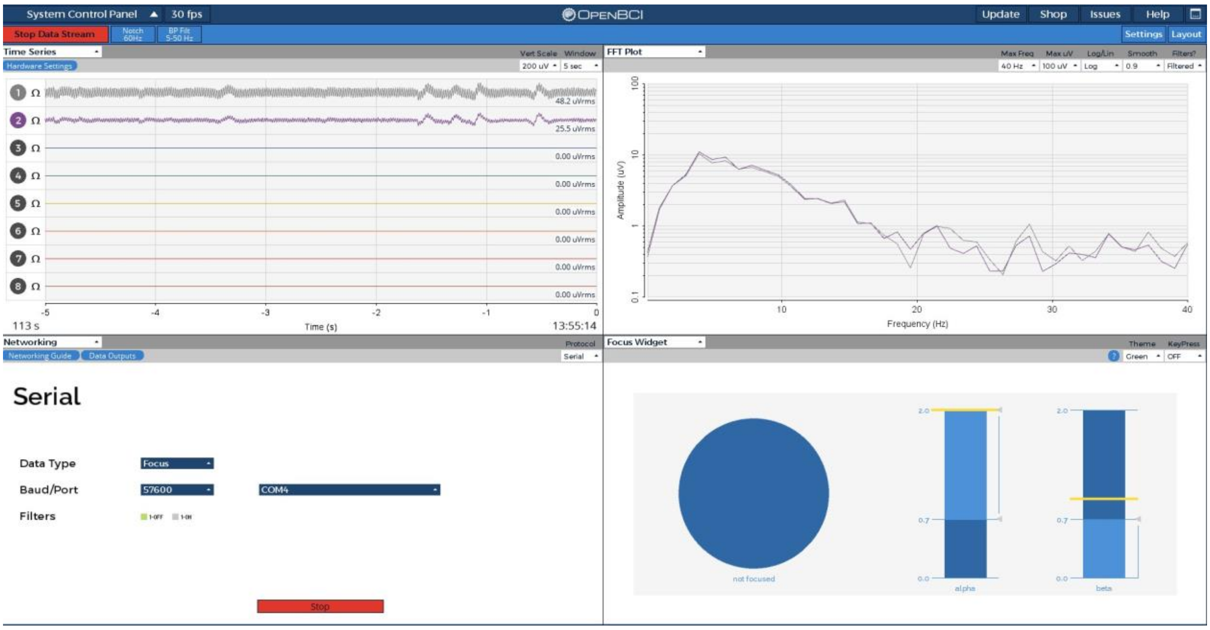

Figure 5.36: OpenBCI GUI plot for when out of the focus state.

5.3.2 Computer window scrolling

Computer window scrolling has been controlled with the data of the brainwave signals. However, for this purpose, the collected data samples have been transmitted by OpenBCI GUI through the networking of the Lab Streaming Layer (LSL). The streamed data signals have been synchronized and further implemented. The control over a window and application has permitted the selection and scrolling through the feed. This has allowed the user to surf through an application or webpage with the focus state of the brainwave frequencies similar to that of the previous section. Figure 5.37 indicates the frequent spikes due to the constant focus and command signals generated in the brain.

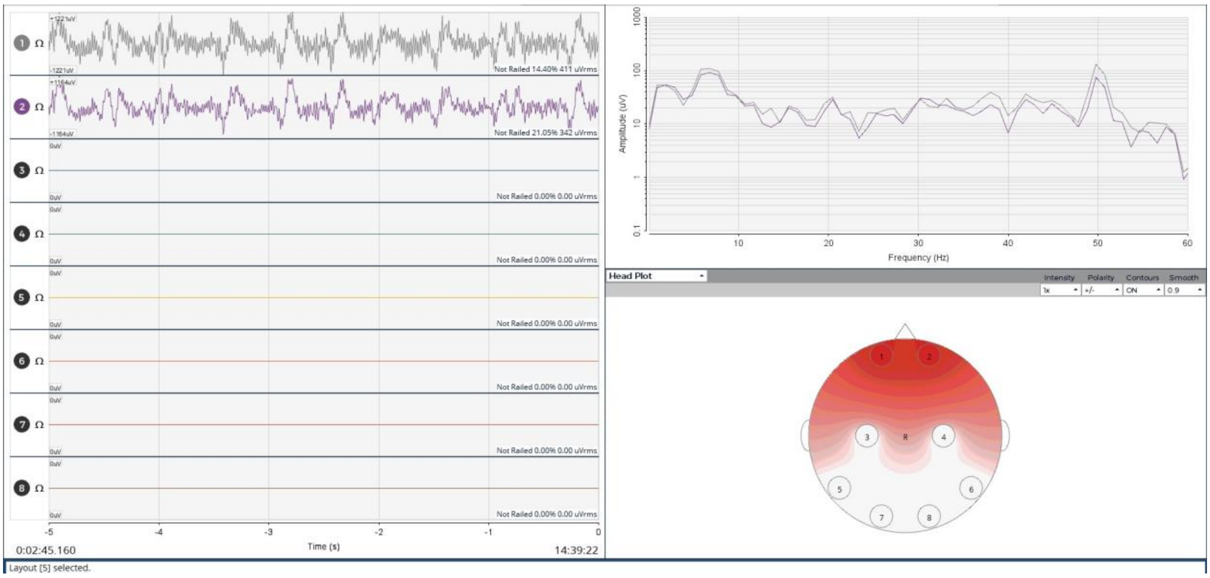

Figure 5.37: OpenBCI GUI plot during computer control and window scrolling.

Chapter 6

Conclusion and Discussion

This chapter addresses the limitations and challenges encountered upon the fulfilment of our project. It further presents the future aspects are remarks that establish the future of our thesis project. Furthermore, the concluding summary provides the notions that we have reached concerning our project.

6.1 Limitations

The preceding segments have emphasized on required procedures for the collective functional assurance of the project. To ensure the aspired performance, the optimum production of brainwaves is an inherent condition. Additionally, the technology demanded is not entirely cost-efficient for developing countries like ours.

Some if not most of the preliminary brain-computer interface (BCI) based researches are based on theoretical hypotheses. This embeds limitations upon practical aspects and applications. Hence, more extended research and funding are required in this field.

Besides, the performance of the brain-computer interfaces (BCI) depends on the accuracy of the electroencephalographic (EEG) data obtained from the measuring channels placed on the scalp [52]. EEG, in general, comprises of complex frequency components. The non-invasive EEG techniques include the variations in external noises and interferences [61]. These noises from the power line and components collaborate with the ones from the brain and artefacts (muscular movements). Conjoined with the original signals, they create disturbances that cause further limitations [72].

The attributes related to the accuracy of the EEG data depends on the subsequent factors [52]:

- Number of measuring channels.
- The amount of data extracted.
- The signal-to-noise ratio (SNR).

Although, we have derived the relevant data after a series of efficient digital signal processing (DSP) techniques, such as [72]:

- Signal filtering using the FIR Butterworth filter.
- Derivation of the significant information with fast Fourier transform (FFT).

However, the partial existence of noise and interferences cause degradation of the collected EEG data samples. To conclude, the SNR adjustments for real-life applications can evidently be the most challenging of all the limitations [52].

6.2 Future aspects of our work

There future aspects of our project include enhancing usability, remote accessibility and application development. The apparent goal is to enhance the usability of the system. As mentioned earlier in the limitations, EEG data acquisition can be enhanced by applying exclusive instrumentation such as the ones used in this [60] paper. We would further be able to investigate the steady-state visual evoked potential (SSVEP) response to an amplitude-modulated visual stimulus and the auditory steady-state response (ASSR) using BCI applications [60].

We further intend to build an application for android mobile phones to improve remote accessibility. This will allow the user to inspect the data streaming in the web-dashboard or mobile application in real-time. Moreover, it can be enhanced for monitoring and alert-system in cases of emergencies. We aim to develop the control of an electric wheelchair implementation by connecting it to the BCI system. The control of wheelchairs using brainwaves can empower mobility in physically challenged and paralysed people. Hence, we would require similar procedures of state-of-the-art machine learning technique as mentioned in the [13] paper. We believe that the comprehensive implementation can be accomplished according to the overall system control implementation shown in figure 5.33 (in chapter 5). We ultimately intend to design our project to be more cost-effective so that affordability assurance can be viable in developing countries like ours.

6.3 Concluding remarks

The fundamental motivation behind this project was to build an assistive device using BCI technology for patients suffering from physical disabilities and paralysis. The primary data observations produced diverse results suggestive of the extensive applications of the accumulated data through the OpenBCI GUI application. To ensure the execution of the performance methodology, we visualised and compared a fewer assortment of data. In presumption upon the learning of the data, we were capable of administering the required ranges for focus-control applications. Hence, similar techniques can be implemented for the cases of impaired patients generating optimum brainwave signals only.

We believe that we are at the initial stage of development of our project since we have been unable to gather data directly from a victim of paralysis. However, as per the discussion in chapter 2, we have ensured that if optimum action potential is perceived in the brainwaves of an individual then our project can assure the performance of our project. The BCI system has innumerable fields of research and application. Hence, for further processing of the data, machine learning and neural networking is imperative. We conclude that, the collective study of Neuroscience and Engineering can inherit beneficial outcomes for the deprived and unfortunate population when governed under a collaborative system.

Bibliography

[1] P. G. Vinoj, S. Jacob, V. G. Menon, S. Rajesh, and M. R. Khosravi, "Brain-Controlled Adaptive Lower Limb Exoskeleton for Rehabilitation of Post-Stroke Paralyzed," IEEE Access, vol. 7, pp. 132628–132648, Jun. 2019, doi: 10.1109/access.2019.2921375.

[2] M. D. Novitasari, A. D. Wibawa, M. H. Purnomo, W. R. Islamiyah and A. Fatoni, "Investigating EEG Pattern During Designed-Hand Movement Tasks in Stroke Patients," 2020 International Seminar on Intelligent Technology and Its Applications (ISITIA), Surabaya, Indonesia, 2020, pp. 141-147, doi: 10.1109/isitia49792.2020.9163680.

[3] "GENDER STATISTICS OF BANGLADESH 2018," Bangladesh Bureau of Statistics (BBS), May-2019. [Online]. Available: http://www.bbs.gov.bd/. [Accessed: 2020].

[4] E. Grabianowski, "How Brain-computer Interfaces Work," HowStuffWorks, 02-Nov-2007. [Online]. Available: https://computer.howstuffworks.com/brain-computer-interface.htm. [Accessed: 20-Oct-2020].

[5] "Electrode Cap Getting Started Guide," OpenBCI Documentation. [Online]. Available: https://docs.openbci.com/docs/04AddOns/01-Headwear/ElectrodeCap. [Accessed: Jan-2021].

[6] J. Best, "What is a brain-computer interface? Everything you need to know about BCIs, neural interfaces and the future of mind-reading computers," ZDNet, 13-Nov-2019. [Online]. Available: https://www.zdnet.com/article/what-is-bci-everything-you-need-to-know-about-brain-computer-interfaces-and-the-future-of-mind-reading-computers/. [Accessed: 21-Oct-2020].

[7] T. T. Contributors, "What is brain-computer interface (BCI)? - Definition from WhatIs.com," WhatIs.com, 22-Mar-2011. [Online]. Available:

https://whatis.techtarget.com/definition/brain-computer-interface-BCI. [Accessed: 24-Oct-2020].

[8] J. J. Shih, D. J. Krusienski, and J. R. Wolpaw, "Brain-Computer Interfaces in Medicine," Mayo Clinic Proceedings, vol. 87, no. 3, pp. 268–279, Feb. 2012, doi: https://doi.org/10.1016/j.mayocp.2011.12.008.

[9] "Disability and health," World Health Organization, 01-Dec-2020. [Online]. Available: https://www.who.int/news-room/fact-sheets/detail/disability-and-health. [Accessed: Dec-2020].

[10] "Assistive devices and technologies," World Health Organization, 19-Oct-2017. [Online]. Available: https://www.who.int/disabilities/technology/en/. [Accessed: 21-Nov-2020].

[11] "Paralysis Management and Treatment," Cleveland Clinic, Feb-2017. [Online]. Available: https://my.clevelandclinic.org/health/diseases/15345-paralysis/management-and-treatment. [Accessed: Dec-2020].

[12] M. Haque and M. E. Murshid, "Disability brief in single chapter and bangladesh perspectives: A rapid overview," Advances in Human Biology, vol. 10, no. 2, p. 41, May 2020, doi: 10.4103/aihb.aihb_6_20.

[13] M. F. Ansari, D. R. Edla, S. Dodia, and V. Kuppili, "Brain-Computer Interface for wheelchair control operations: An approach based on Fast Fourier Transform and On-Line Sequential Extreme Learning Machine," Clinical Epidemiology and Global Health, vol. 7, no. 3, pp. 274–278, Sep. 2019, doi: 10.1016/j.cegh.2018.10.007.

[14] J. Eske, “Paralysis: Types, symptoms, and treatment,” Medical News Today, 02-Apr-2020. [Online]. Available: https://www.medicalnewstoday.com/articles/paralysis. [Accessed: 08-Dec-2020].

[15] “Paralysis: Causes, Symptoms, Diagnosis & Treatment,” Cleveland Clinic, 2020. [Online]. Available: https://my.clevelandclinic.org/health/diseases/15345-paralysis#:~:text=In%20most%20cases%2C%20people%20get,Spinal%20cord%20injury. [Accessed: Dec-2020].

[16] Technology Networks, “The Electric Signals That Make the Human Brain Unique,” Neuroscience from Technology Networks, 19-Oct-2018. [Online]. Available: https://www.technologynetworks.com/neuroscience/news/the-electric-signals-that-make-the-human-brain-unique-310800. [Accessed: 30-Nov-2020].

[17] D. S. Peterka, H. Takahashi, and R. Yuste, “Imaging Voltage in Neurons,” Neuron, vol. 69, no. 1, pp. 9–21, Jan. 2011, doi: 10.1016/j.neuron.2010.12.010.

[18] A. Raj and S. M. Jaisakthi, “Analysis of Brain Wave Due to Stimulus Using EEG,” 2018 International Conference on Computer, Communication, and Signal Processing (ICCCSP), Chennai, 2018, doi: 10.1109/ICCCSP.2018.8452823.

[19] Zhongming Liu, Lei Ding and Bin He, “Integration of EEG/MEG with MRI and fMRI,” in IEEE Engineering in Medicine and Biology Magazine, vol. 25, no. 4, pp. 46-53, July-Aug. 2006, doi: 10.1109/MEMB.2006.1657787.

[20] S. Jain, R. Mittra, and J. Wiart, “FULL WAVE MODELING OF BRAIN WAVES AS ELECTROMAGNETIC WAVES (Invited Paper),” Progress In Electromagnetics Research, vol. 151, pp. 95–107, 2015, doi: 10.2528/pier15011404.

[21] S. Kieffer, "How the Brain Works: Johns Hopkins Comprehensive Brain Tumor Center," How the Brain Works | Johns Hopkins Comprehensive, 03-Dec-2018. [Online]. Available: https://www.hopkinsmedicine.org/neurology_neurosurgery/centers_clinics/brain_tumor/about-brain-tumors/how-the-brain-works.html. [Accessed: 30-Oct-2020].

[22] "How does the brain work?," InformedHealth.org [Internet]., 31-Oct-2018. [Online]. Available: https://www.ncbi.nlm.nih.gov/books/NBK279302/. [Accessed: 07-Dec-2020].

[23] S. Genon, A. Reid, R. Langner, K. Amunts, and S. B. Eickhoff, "How to Characterize the Function of a Brain Region," Trends in Cognitive Sciences, vol. 22, no. 4, pp. 350–364, Feb. 2018, doi: https://doi.org/10.1016/j.tics.2018.01.010.

[24] B. Cuffari, "The Anatomy of the Human Brain," News, 20-Dec-2020. [Online]. Available: https://www.news-medical.net/health/The-Anatomy-of-the-Human-Brain.aspx. [Accessed: 12-Dec-2020].

[25] K. A. Maldonado and K. Alsayouri, "Physiology, Brain," StatPearls [Internet]., 24-May-2020. [Online]. Available: https://www.ncbi.nlm.nih.gov/books/NBK551718/. [Accessed: 15-Dec-2020].

[26] "Brain Anatomy, Anatomy of the Human Brain," mayfieldclinic.com, Apr-2018. [Online]. Available: https://mayfieldclinic.com/pe-anatbrain.htm. [Accessed: 19-Dec-2020].

[27] M. W. Richardson, "How Much Energy Does the Brain Use?," BrainFacts.org, 01-Feb-2019. [Online]. Available: https://www.brainfacts.org/brain-anatomy-and-function/anatomy/2019/how-much-energy-does-the-brain-use-020119. [Accessed: 20-Dec-2020].

[28] S. Jimsheleishvili, "Neuroanatomy, Cerebellum," StatPearls [Internet]., 31-Jul-2020. [Online]. Available: https://www.ncbi.nlm.nih.gov/books/NBK538167/. [Accessed: 23-Dec-2020].

[29] "What are the Brain Waves Frequencies?," Neuro Clinic. [Online]. Available: http://neuroclinicbarrie.com/neurofeedback/links-resources/brain-waves-frequencies/. [Accessed: 28-Nov-2020].

[30] T. Das, "Brain waves create consciousness," International Journal of Development Research, vol. 08, Jun. 2018. [Accessed: 17-Nov-2020].

[31] "Cyton Biosensing Board (8-channels)," OpenBCI Online Store. [Online]. Available: https://shop.openbci.com/collections/frontpage/products/cyton-biosensing-board-8-channel?variant=38958638542. [Accessed: Jan-2021].

[32] "ADS1299-x Low-Noise, 4-, 6-, 8-Channel, 24-Bit, Analog-to ...," Texas Instruments, Jan-2017. [Online]. Available: https://www.ti.com/lit/ds/symlink/ads1299.pdf. [Accessed: Jan-2021].

[33] "PIC32MX250F128B - Microcontrollers and Processors," MICROCHIP. [Online]. Available: https://www.microchip.com/wwwproducts/en/en557425. [Accessed: Nov-2020].

[34] "Cyton Data Format," OpenBCI Documentation. [Online]. Available: https://docs.openbci.com/docs/02Cyton/CytonDataFormat. [Accessed: Jan-2021].

[35] " FT231X – Full Speed USB to Full Handshake UART," FTDI Chip. [Online]. Available: https://www.ftdichip.com/Products/ICs/FT231X.html. [Accessed: Jan-2021].

[36] "OpenBCI WiFi," OpenBCI Documentation. [Online]. Available: https://docs.openbci.com/docs/05ThirdParty/03-WiFiShield/WiFiLanding. [Accessed: Jan-2021].

[37] “OpenBCI WiFi Shield API · OpenBCI Documentation,” OpenBCI Documentation. [Online]. Available: https://docs.openbci.com/docs/05ThirdParty/03-WiFiShield/WiFiAPI. [Accessed: Jan-2021].

[38] “ESP8266EX Datasheet,” Espressif Systems, 2020. [Online]. Available: https://www.espressif.com/en/subscribe. [Accessed: 2021].

[39] B. Meneses-Claudio, W. Alvarado-Diaz, and A. Roman-Gonzalez, “Differentiation of Brain Waves from the Movement of the Upper and Lower Extremities of the Human Body,” International Journal of Advanced Computer Science and Applications, vol. 9, no. 11, 2018, doi: 10.14569/ijacsa.2018.091167.

[40] “What are Brainwaves?: Improve Brain Health with Neurofeedback,” Sinha Clinic, 25-Aug-2020. [Online]. Available: https://www.sinhaclinic.com/what-are-brainwaves/. [Accessed: Nov-2020].

[41] MIT, “Controlling attention with brain waves,” ScienceDaily, 04-Dec-2019. [Online]. Available: https://www.sciencedaily.com/releases/2019/12/191204145752.htm. [Accessed: Nov-2020].

[42] B. Farnsworth, “EEG vs. MRI vs. fMRI - What are the Differences?,” imotions, 12-Jul-2019. [Online]. Available: https://imotions.com/blog/eeg-vs-mri-vs-fmri-differences/. [Accessed: 05-Nov-2020].

[43] M. D. Peter Pressman, “How Does a Functional MRI Machine Work?,” Verywell Health, 31-Jan-2020. [Online]. Available: https://www.verywellhealth.com/what-is-functional-magnetic-resonance-imaging-2488813. [Accessed: 18-Dec-2020].

[44] M. E. Raichle, “Two views of brain function,” Trends in Cognitive Sciences, vol. 14, no. 4, pp. 180–190, Mar. 2010, doi: 10.1016/j.tics.2010.01.008.

[45] "Electroencephalogram (EEG)," Johns Hopkins Medicine, 2020. [Online]. Available: https://www.hopkinsmedicine.org/health/treatment-tests-and-therapies/electroencephalogram-eeg. [Accessed: Dec-2020].

[46] M. Khazi, A. Kumar, and V. M J, "Analysis of EEG Using 10:20 Electrode System," International Journal of Innovative Research in Science, Engineering and Technology, vol. 1, no. 2, Dec. 2012.

[47] T. Ball, M. Kern, I. Mutschler, A. Aertsen, and A. Schulze-Bonhage, "Signal quality of simultaneously recorded invasive and non-invasive EEG," NeuroImage, vol. 46, no. 3, pp. 708–716, Mar. 2009, doi: 10.1016/j.neuroimage.2009.02.028.

[48] "Python and OpenBCI," OpenBCI Documentation. [Online]. Available: https://docs.openbci.com/docs/09Deprecated/Python. [Accessed: 01-Jan-2021].

[49] D. Xiao, "Comparison of Three Motor Imagery EEG Signal Processing Methods," Advances in Intelligent and Soft Computing Advances in Multimedia, Software Engineering and Computing, vol. 2, pp. 503–508, 2011, doi: https://doi.org/10.1007/978-3-642-25986-9_79.

[50] T. D. Papageorgiou, J. M. Lisinski, M. A. McHenry, J. P. White, and S. M. LaConte, "Brain-computer interfaces increase whole-brain signal to noise," Proceedings of the National Academy of Sciences, vol. 110, no. 33, pp. 13630–13635, Aug. 2013, doi: 10.1073/pnas.1210738110.

[51] X. Zhang, L. Yao, X. Wang, J. Monaghan, D. McAlpine, and Y. Zhang, "A Survey on Deep Learning-based Non-Invasive Brain Signals: Recent Advances and New Frontiers," Journal of Neural Engineering, Oct. 2020, DOI: 10.1145/1122445.1122456.

[52] D. Gutierrez, “Designing a spatial filter to improve SNR in two-class discrimination problems for BCI applications,” 2008 42nd Asilomar Conference on Signals, Systems and Computers, Pacific Grove, CA, 2008, doi: 10.1109/ACSSC.2008.5074428.

[53] J. Vasković, “Action potential,” Kenhub, 29-Oct-2020. [Online]. Available: https://www.kenhub.com/en/library/anatomy/action-potential. [Accessed: 26-Dec-2020].

[54] “Fast Fourier transform,” Fast Fourier transform - Competitive Programming Algorithms. [Online]. Available: https://cp-algorithms.com/algebra/fft.html#toc-tgt-2. [Accessed: 28-Dec-2020].

[55] F. Zhang, C. Han, L. Li, X. Zhang, J. Xie, and Y. Li, “Research on High-Frequency Combination Coding-Based SSVEP-BCIs and Its Signal Processing Algorithms,” Shock and Vibration, vol. 2015, Sep. 2015, doi: 10.1155/2015/194230.

[56] R. C. Gonzalez and R. E. Woods, Digital image processing, 3rd ed. New York: Pearson Education International., 2018.

[57] S. Haykin, Introduction to analog and digital communications, 2nd ed. United States of America: John Wiley Sons, Inc., 2016.

[58] C. E. Shannon, “A Mathematical Theory of Communication,” The Bell System Technical Journal, vol. 27, no. 4, pp. 379–423; 623-656, Oct. 1948, doi: 10.1002/j.1538-7305.1948.tb00917.x.

[59] E. Por, M. V. Kooten, and V. Sarkovic, “Nyquist–Shannon sampling theorem,” May 2019.

[60] H. J. Baek, M. H. Chang, J. Heo, and K. S. Park, “Enhancing the Usability of Brain-Computer Interface Systems,” Computational Intelligence and Neuroscience, vol. 2019, pp. 1–12, Jun. 2019, doi: 10.1155/2019/5427154.

[61] A. Suarez-Perez, G. Gabriel, B. Rebollo, X. Illa, A. Guimerà-Brunet, J. Hernández-Ferrer, M. T. Martínez, R. Villa, and M. V. Sanchez-Vives, “Quantification of Signal-to-Noise Ratio in Cerebral Cortex Recordings Using Flexible MEAs With Co-localized Platinum Black, Carbon Nanotubes, and Gold Electrodes,” Frontiers in Neuroscience, vol. 12, Nov. 2018, doi: 10.3389/fnins.2018.00862.

[62] S. Paonessa, “Reducing Signal Noise in Practice,” Precision Digital. [Online]. Available: https://www.predig.com/whitepaper/reducing-signal-noise-practice. [Accessed: 01-Jan-2021].

[63] C. Bedoya, D. Estrada, S. Trujillo, N. Trujillo, D. Pineda and J. D. López, “Automatic component rejection based on fuzzy clustering for noise reduction in electroencephalographic signals,” Symposium of Signals, Images and Artificial Vision - 2013: STSIVA - 2013, Bogota, 2013, doi: 10.1109/stsiva.2013.6644922.

[64] S. W. Smith, The scientist and engineer's guide to digital signal processing. San Diego, CA: California Technical Pub., 1997. [Accessed: 03-Jan-2021].

[65] H. Hindarto and S. Sumarno, “Feature Extraction of Electroencephalography Signals Using Fast Fourier Transform,” CommIT (Communication and Information Technology) Journal, vol. 10, no. 2, pp. 49–52, Oct. 2016, doi: 10.21512/commit.v10i2.1548.

[66] R. Keim, “The Nyquist–Shannon Theorem: Understanding Sampled Systems - Technical Articles,” All About Circuits, 06-May-2020. [Online]. Available: https://www.allaboutcircuits.com/technical-articles/nyquist-shannon-theorem-understanding-sampled-systems/. [Accessed: 04-Jan-2021].

[67] “The Nyquist-Shannon Sampling Theorem,” in EECS20N: Signals and Systems. [Online]. Available: https://ptolemy.berkeley.edu/eecs20/week13/nyquistShannon.html. [Accessed: 04-Jan-2021].

[68] "Band Pass Filter - Passive RC Filter Tutorial," Basic Electronics Tutorials, 15-May-2018. [Online]. Available: https://www.electronics-tutorials.ws/filter/filter_4.html. [Accessed: 04-Jan-2021].

[69] A. Gunjal, S. R. Gagare, and R. P. Labade, "Bandwidth enhancement in band pass filter (BPF) using microstrip couple lines for WLAN (2.4GHZ) applications," 2016 International Conference on Electrical, Electronics, and Optimization Techniques (ICEEOT), Chennai, Mar. 2016, doi: 10.1109/iceeot.2016.7755383.

[70] "What is a Notch Filter?," everything RF, 29-Aug-2018. [Online]. Available: https://www.everythingrf.com/community/what-is-a-notch-filter. [Accessed: 06-Jan-2021].

[71] "Notch Filter (Band-Stop): What is it? (Circuit, Design & Transfer Function)," Electrical4U, 11-Oct-2020. [Online]. Available: https://www.electrical4u.com/band-stop-notch-filter/#:~:text=A%20notch%20filter%20. [Accessed: 03-Jan-2021].

[72] Shakshi and R. Jaswal, "Brain Wave Classification and Feature Extraction of EEG Signal by Using FFT on Lab View," International Research Journal of Engineering and Technology (IRJET), vol. 03, no. 07, pp. 1208–1212, Jul. 2016, doi: https://www.irjet.net/

[73] X. Qian, Y. P. Xu, and X. Li, "A CMOS Continuous-Time Low-Pass Notch Filter for EEG Systems," Analog Integrated Circuits and Signal Processing, vol. 44, no. 3, pp. 231–238, Sep. 2005, doi: 10.1007/s10470-005-3007-x.

[74] "Op Amp Active Notch Filter Circuit," Electronics Notes. [Online]. Available: https://www.electronics-notes.com/articles/analogue_circuits/operational-amplifier-op-amp/notch-filter-active-circuit.php. [Accessed: Dec-2020].

[75] “GUI Widget Guide,” OpenBCI Documentation. [Online]. Available: https://docs.openbci.com/docs/06Software/01-OpenBCISoftware/GUIWidgets#serial. [Accessed: 09-Dec-2020].

[76] “Butterworth Filter Design and Low Pass Butterworth Filters,” Basic Electronics Tutorials, 24-Jul-2018. [Online]. Available: https://www.electronics-tutorials.ws/filter/filter_8.html. [Accessed: 05-Jan-2021].

[77] “GUI Widget Guide,” OpenBCI Documentation. [Online]. Available: https://docs.openbci.com/docs/06Software/01-OpenBCISoftware/GUIWidgets#lsl. [Accessed: 01-Jan-2021].

[78] “The Lobes and Limbic System,” My-MS.org. [Online]. Available: https://my-ms.org/anatomy_brain_part2.htm. [Accessed: 01-Jan-2021].

[79] “GUI Widget Guide,” OpenBCI Documentation. [Online]. Available: https://docs.openbci.com/docs/06Software/01-OpenBCISoftware/GUIWidgets#types-of-waves. [Accessed: 02-Jan-2021].

[80] “Reusable EEG Cup Electrode Gold and Silver,” Technomed medical accessories. [Online]. Available: https://technomed.nl/sites/default/files/product/downloads/T-2019-008.01_EN-Reusable_EEG_Cup_Electrode_Gold_and_Silver_Product_Datasheet-Digital.pdf. [Accessed: Dec-2020].

[81] “Gold Cup Electrodes,” OpenBCI Online Store. [Online]. Available: https://shop.openbci.com/products/openbci-gold-cup-electrodes?variant=37345591591070. [Accessed: 09-Nov-2020].

[82] "Ten20 Conductive Paste 2oz jars pack of 3," OpenBCI Online Store. [Online]. Available: https://shop.openbci.com/collections/frontpage/products/ten20-conductive-paste-2oz-jars?variant=31373533198. [Accessed: Dec-2020].

[83] "Electrode Cap Gel," OpenBCI Online Store. [Online]. Available: https://shop.openbci.com/collections/frontpage/products/electrodegel?variant=28056992776264. [Accessed: Oct-2020].

[84] "EMG/ECG Foam Solid Gel Electrodes (30/pack)," OpenBCI Online Store. [Online]. Available: https://shop.openbci.com/collections/frontpage/products/skintact-f301-pediatric-foam-solid-gel-electrodes-30-pack?variant=29467659395. [Accessed: Nov-2020].

[85] "EMG/ECG Snap Electrode Cables," OpenBCI Online Store. [Online]. Available: https://shop.openbci.com/collections/frontpage/products/emg-ecg-snap-electrode-cables?variant=37345654046878. [Accessed: Jan-2021].

[86] "Motor driver L298N." [Online]. Available: https://images-na.ssl-images-amazon.com/images/I/61VkNn0PcaL._AC_SL1000_.jpg. [Accessed: 2021].

[87] "DUAL FULL-BRIDGE DRIVER," ST. [Online]. Available: http://www.st.com. [Accessed: Jan-2021].

[88] "The OpenBCI GUI," OpenBCI Documentation. [Online]. Available: https://docs.openbci.com/docs/06Software/01-OpenBCISoftware/GUIDocs#data-log-options. [Accessed: Jan-2021].

[89] B. S. Armour, E. A. Courtney-Long, M. H. Fox, H. Fredine, and A. Cahill, "Prevalence and Causes of Paralysis—United States, 2013," American Journal of Public Health, vol. 106, no. 10, pp. 1855–1857, 2016, doi: 10.2105/ajph.2016.303270.

Appendix A.

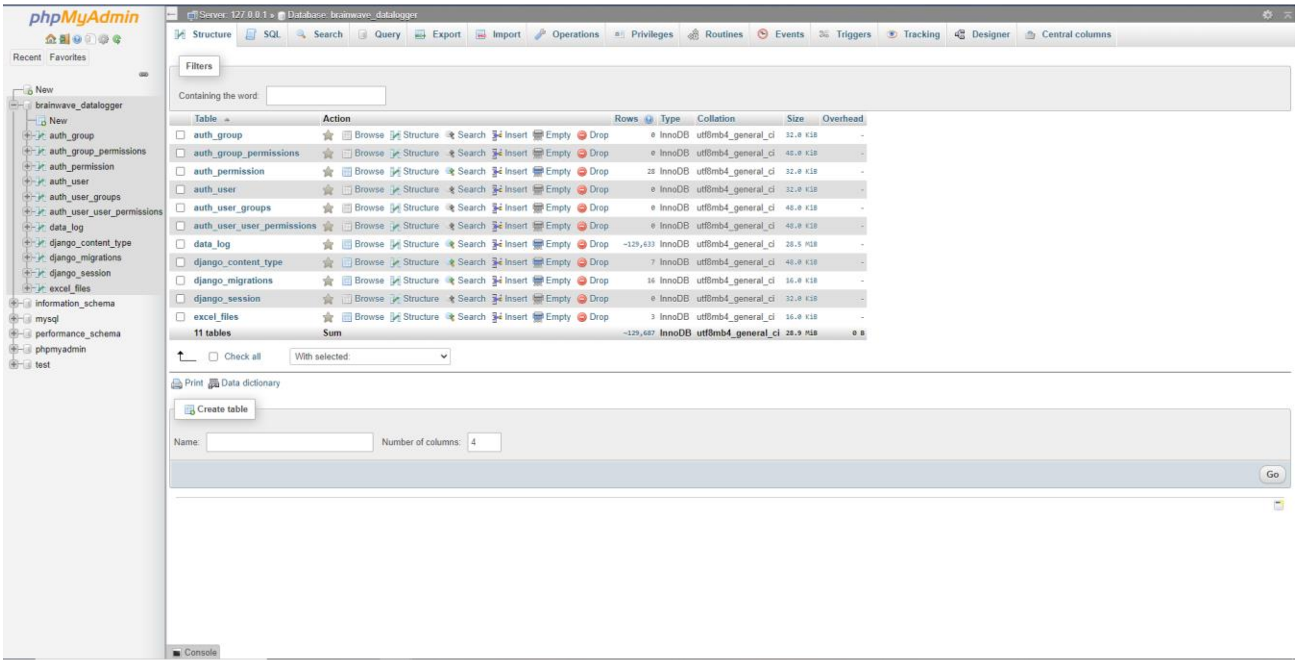
phpMyAdmin
Recent Favorites
New
brainwave_datalogger
New
auth_group
auth_group_permissions
auth_permission
auth_user
auth_user_groups
auth_user_user_permissions
data_log
django_content_type
django_migrations
django_session
excel_files
information_schema
mysql
performance_schema
phpmyadmin
test
Server: 127.0.0.1 » Database: brainwave_datalogger
Structure SQL Search Query Export Import Operations Privileges Routines Events Triggers Tracking Designer Central columns
Filters
Containing the word:
Table Action Rows Type Collation Size Overhead
auth_group Browse Structure Search Insert Empty Drop 0 InnoDB utf8mb4_general_ci
auth_group_permissions Browse Structure Search Insert Empty Drop 0 InnoDB utf8mb4_general_ci
auth_permission Browse Structure Search Insert Empty Drop 28 InnoDB utf8mb4_general_ci
auth_user Browse Structure Search Insert Empty Drop 0 InnoDB utf8mb4_general_ci
auth_user_groups Browse Structure Search Insert Empty Drop 0 InnoDB utf8mb4_general_ci
auth_user_user_permissions Browse Structure Search Insert Empty Drop 0 InnoDB utf8mb4_general_ci
data_log Browse Structure Search Insert Empty Drop InnoDB utf8mb4_general_ci
django_content_type Browse Structure Search Insert Empty Drop 7 InnoDB utf8mb4_general_ci
django_migrations Browse Structure Search Insert Empty Drop 16 InnoDB utf8mb4_general_ci
django_session Browse Structure Search Insert Empty Drop 0 InnoDB utf8mb4_general_ci
excel_files Browse Structure Search Insert Empty Drop 3 InnoDB utf8mb4_general_ci
11 tables Sum InnoDB utf8mb4_general_ci
Check all
With selected:
Print Data dictionary
Create table
Name:
Number of columns: 4
Go
Console